Research Article

Risk Assessment of Constructing Deep Foundation Pits for Metro Stations Based on Fuzzy Evidence Reasoning and Two-tuple Linguistic Analytic Network Process

Jie Jiang [1,2,3] **Guangyang Liu,** [1,2,3] **Xi Huang,** [1,2,3] **and Xiaoduo Ou** [1,2,3]

[1] *College of Civil Engineering and Architecture, Guangxi University, Nanning 530004, China*
[2] *Key Laboratory of Disaster Prevention and Structural Safety of Ministry of Education, Guangxi University,*
Nanning 530004, China
[3] *Guangxi Key Laboratory of Disaster Prevention and Engineering Safety, Guangxi University, Nanning 530004, China*

Correspondence should be addressed to Jie Jiang; 183455216@qq.com

Accidents occur frequently while constructing deep foundation pits for metro stations, thereby risking substantial economic losses and casualties. To subject the construction of such pits to scientific and rational risk assessment and overcome the limitations of existing risk evaluation models and risk fusion problems, proposed here is a risk-assessment model for such pits based on fuzzy evidential reasoning and the two-tuple linguistic analytic network process (TL-ANP). First, the risk loss indicators are optimized, the weights of different risk events and of each risk loss indicator in the metro-station deep-foundation-pit construction project are calculated using TL-ANP, and trapezoidal fuzzy numbers are used to describe the occurrence probability of each risk event and loss. Second, relying on a table of expert weight indices, the best–worst method based on generalized interval-valued trapezoidal fuzzy numbers is used to determine the weights of experts. Finally, the overall risk grade of the construction project is evaluated by aggregating the risk levels of all risk events through an evidence-reasoning algorithm. The analysis results for a deep foundation pit for a station on Line 5 of Nanning Metro show that the model provides a quantitative basis for determining expert weights and risk loss weights reasonably and improving the reliability of the evaluation system. Also, not only does applying the method show that such a construction project can be judged as having a certain risk grade, but more importantly it can identify the key factors and loss indicators affecting the overall risk grade of the pit, whereupon risk control measures can be adopted in a targeted manner. In comparison with traditional methods, the proposed method is shown to be practical and effective, providing a reference basis for analyzing the risks of similar projects in the future and guaranteeing construction safety.

1. Introduction

Constructing deep foundation pits (DFPs) is an essential but high-risk part of any urban rail project, and the uncertain factors in the construction process are the essential reasons for the risks in metro DFP construction. During the construction of a metro DFP, complex geological conditions and the surrounding environment often lead to large-scale destructive accidents [1, 2]. For example, while constructing Xianghu station on Line 1 of Hangzhou Metro in 2008, the DFP collapsed because of severe overexcavation and failure of the supporting system, resulting in more than 20 deaths

[3]. Between 2003 and 2017, there were 322 metro construction accidents in Guangdong and Beijing in China, with an average fatality rate of 89.4%. Given that in the past decade, the total infrastructure investment in China's metro projects was ca. RMB 4080 billion, the ability to make timely and objective assessments of the construction risks of metro DFPs is pertinent to not only safety and maintenance costs but also safeguarding the safety of construction workers and residents, and risk management for metro DFP construction is now of high priority in China [3].

Existing evaluation methods derived from probabilistic risk analysis, such as fault tree analysis and Monte Carlo

simulation, have greatly promoted the development of risk management for metro DFP construction. However, the existing assessment methods based on probabilistic risk analysis have several drawbacks; their evaluation results depend heavily on the completeness and accuracy of the risk data, meaning that these methods often fail to give satisfactory results [4, 5]. Therefore, to overcome the inherent defects of these methods based on probability theory, many scholars have adopted a series of fuzzy evaluation methods to assess the risk of metro DFP construction. Wang and Chen [6] combined fuzzy comprehensive evaluation and Bayesian networks to evaluate the risks of DFP projects in terms of risk probability, loss, and controllability, and Meng et al. [1] applied hierarchical analysis and fuzzy set theory to evaluating the risks of DFP supports. However, these fuzzy evaluation methods lack a reasonable way to determine the weights of experts, which is the key to collecting expert evaluation information. The best-worst method (BWM) performs well in reducing the number of pairwise comparisons and maintaining judgment consistency [7], and it has received increasing attention for resolving expert weights.

The overall construction risk of a metro DFP comprises many subrisks combined in different ways, and each subrisk has a complex interdependence. To analyze comprehensively the overall impact of many risk events on the whole system, a large amount of risk information must be fused to determine the overall risk of metro DFP construction. The method of fuzzy evidential reasoning (FER) involves modeling the risk uncertainty by combining fuzzy set theory and belief structure, realizing risk information fusion through an FER algorithm, and finally obtaining evaluation results with different belief grades [8]. Du et al. [9] first used fuzzy evidence theory to evaluate comprehensively the construction risk of DFP engineering in 2014; the evaluation results reflected the beliefs of experts about the risk grade, but the method failed to solve the risk-assessment problem when more than two continuous fuzzy evaluation grades intersected. Wei et al. [10] proposed a new belief-structure transformation method for cases in which the evaluation grade is a multi-intersection fuzzy state, but they failed to consider multiple risk evaluation indicators and their weights. Also, determining the weight of each risk event is an important part of integrating all the risk information, but previous single-risk evaluation methods struggle to analyze reasonably the weight relationship of each risk event in metro DFP construction; for example, the model constructed by the analytic hierarchy process (AHP) is a recursive hierarchy and is unsuitable for systems with complex levels [11–13], fuzzy comprehensive evaluation is very subjective in determining the weight of each risk in the evaluation object [14, 15], and fuzzy network analysis cannot avoid information loss or distortion [16]. Therefore, there is an urgent need to find a suitable method for determining the weight of each risk event for a metro DFP construction risk system.

To address the above shortcomings, established herein is a new risk-assessment model for metro DFPs based on the two-tuple linguistic analytic network process (TL-ANP) and

FER; this model optimizes expert weights and risk event weights and refines the loss evaluation indicators in fuzzy language. We then apply it to the engineering example of a DFP for a metro station on Line 5 of Nanning Metro, which offers a reference basis for future risk analysis of similar projects. The present research results can be used in the risk management of constructing actual metro DFP projects to ensure construction safety and reduce potential losses.

2. Basic Theory

2.1. Fuzzy Evidential Reasoning (FER).
Fuzzy set theory [17] is used widely in model recognition, risk assessment, and uncertain decision making. In different stages of DFP construction, the information that can be collected for risk assessment is often fuzzy, and fuzzy set theory can better quantify risk assessment by transforming experts' subjective linguistic fuzzy judgments into fuzzy numbers. The present study uses trapezoidal fuzzy numbers, which are more suitable for risk assessment in engineering construction.

Liu et al. [18] proposed that FER is a safety analysis framework that combines evidential fuzzy set theory and evidential reasoning, and it is commonly used to deal with fuzziness or fuzzy uncertainty in fuzzy assessment problems. For an evaluation of the indicators, suppose that the risk event is $e_l (l = 1, 2, \ldots, L)$, the weight is $\lambda = (\lambda_1, \lambda_2, \ldots \lambda_L)$, and the risk grade is $H = \{H_n, n = 1, 2, \ldots N\}$. The general steps of fuzzy evaluation using the FER method can be found in the evidence fusion method of Yang et al. [19].

First, the results of expert scoring in the form of trapezoidal fuzzy numbers should be converted into a belief structure $\{(H_n, \gamma_n^l), n = 1, 2 \ldots N\}$, where γ_n^l is the evidence for the object to be evaluated as H_n on evaluation indicator e_l, which satisfies $\gamma_n^l \geq 0$ and $\sum \gamma_n^l \leq 1$. Then, all the evidence is merged using an FER algorithm, which is used to calculate β_n and $\beta_{n,(n+1)}$, where β_n is the belief in the evaluation target as a whole being rated as H_n, $\beta_{n,(n+1)}$ is the belief in the evaluation target being rated as H_n or H_{n+1} (i.e., there is an intersection of fuzzy evaluation grades), and $\beta_{n,(n+1)}$ must be allocated to β_n and β_{n+1}. Finally, the distributed belief and the previously obtained belief β_n are superimposed to obtain the final result $\{(H_n, \beta_n), n = 1, 2 \ldots N\}$ of the fuzzy evaluation of the evaluation object.

2.2. Model of Generalized Linguistic-Values Two-Tuple.
Martinez and Herrera [20] proposed a model of a linguistic-values two-tuple, which represented discrete language information as a continuous language-valued model, thus overcoming the problem of information loss in a continuous domain. Chen and Tai [21] proposed a model of a generalized linguistic-values two-tuple and a conversion function, which overcomes the defect of the uncertain value range of β. If $S = \{s_0, s_1, s_2, \ldots, s_g\}$ is a discrete set of odd-dimensional linguistic terms, then (s_i, α) is a linguistic two-tuple value and β is the linguistic two-tuple value's representative value. β represents the result of the language symbol assembly

operation, and the linguistic two-tuple values corresponding to β can be obtained by the reversible function Δ:

$$\Delta: [0,1] \longrightarrow S \times \left[-\frac{1}{2g}, \frac{1}{2g}\right), \tag{1}$$

$$\Delta(\beta) = (s_i, \alpha).$$

where $i = \text{round}(\beta \cdot g)$, $\alpha = \beta - (i/g)$, $\alpha \in (-(1/2g), (1/2g))$, and

$$\Delta^{-1}: S \times \left[-\frac{1}{2g}, \frac{1}{2g}\right) \longrightarrow [0,1],$$

$$\Delta^{-1}(s_i, \alpha) = \frac{i}{g} + \alpha \tag{2}$$

$$= \beta.$$

2.3. Two-Tuple Linguistic Analytic Network Process (TL-ANP). Many scholars use the fuzzy analytic network process to determine risk factor weights, but there is information loss in the process of converting language scores into triangular fuzzy numbers [22]. To make up for this deficiency, Wan et al. [16] used linguistic variables to represent the scores for pairwise comparisons of risk sets and subrisks, capturing the uncertainty in pairwise comparison judgments. Therefore, herein TL-ANP is used to evaluate the weight of risk factors. Classical ANP is extended by using linguistic variables to replace the numerical values of the 1–9 scale, and the underlying ideas are as follows:

First, linguistic two-tuple values are used to compare risk factors in pairs to form a pairwise judgment matrix. Second, the Eigenroot method is used to determine the weight vector of the judgment matrix. Finally, the weight vector is processed and integrated to obtain a supermatrix. Using a similar method, the factor-set weight matrix can be obtained, and then the limit value of the weighted supermatrix is calculated to obtain the normalized weight value of each risk factor. For the specific steps, see Section 4.3.

2.4. Generalized Interval-Valued Trapezoidal Fuzzy Best–Worst Method (GITrF-BWM). BWM has become a popular method for solving multicriteria decision-making problems because of its efficiency in reducing the number of pairwise comparisons and its good performance in maintaining judgment consistency [23, 24]. Wan et al. [7] proposed a new GITrF-BWM based on generalized interval-valued trapezoidal fuzzy numbers (GITrFNs). In this approach, decision makers identify the best and worst experts in a given situation; then according to the pairwise comparison, the weight of the expert is obtained. The specific steps are as follows:

Step 1: Determine the expert set $S = \{s_1, s_2, ..., s_n\}$.

Step 2: Decision makers decide who is the best expert s_B and the worst expert s_w.

Step 3: Establish the corresponding relationships between the linguistic terms and the GITrFNs. (see Table 1).

Step 4: Provide the linguistic reference preferences for the best expert, and obtain the GITrF best-expert-to-other-experts vector $\widetilde{G}_B = [\widetilde{g}_{B1}, \widetilde{g}_{B2}, \widetilde{g}_{B3}, \ldots, \widetilde{g}_{Bn}]$, where $\widetilde{g}_{Bj} = [(g^l_{1Bj}, g^l_{2Bj}, g^l_{3Bj}, g^l_{4Bj}; h^l_{gBj}), (g^u_{1Bj}, g^u_{2Bj}, g^u_{3Bj}, g^u_{4Bj}; h^u_{gBj})]$.

Step 5: Provide the linguistic reference preferences for the worst expert, and obtain the GITrF other-experts-to-worst-expert vector $\widetilde{G}_W = [\widetilde{g}_{1W}, \widetilde{g}_{2W}, \ldots, \widetilde{g}_{nW}]$, where $\widetilde{g}_{jW} = [(g^l_{1jW}, g^l_{2jW}, g^l_{3jW}, g^l_{4jW}; h^l_{gjW}), (g^u_{1jW}, g^u_{2jW}, g^u_{3jW}, g^u_{4jW}; h^u_{gjW})]$.

Step 6: Let the optimal GITrF weight vector for experts be $\widetilde{w}_j = [(w^l_{1j}, w^l_{2j}, w^l_{3j}, w^l_{4j}; h^l_{wj}), (w^u_{1j}, w^u_{2j}, w^u_{3j}, w^u_{4j}; h^u_{wj})]$, which can be solved by establishing the following programming model:

$$\min_j \max\left\{\left|\frac{\widetilde{w}_B}{\widetilde{w}_j} - \widetilde{g}_{Bj}\right|, \left|\frac{\widetilde{w}_j}{\widetilde{w}_w} - \widetilde{g}_{jW}\right|\right\}$$

$$\text{s.t.} \begin{cases} w^l_{1j} \leq w^l_{2j} \leq w^l_{3j} \leq w^l_{4j}, \\ w^u_{1j} \leq w^u_{2j} \leq w^u_{3j} \leq w^u_{4j}, \\ \sum_{j=1}^n R(\widetilde{w}_j) = 1, \; w^l_{4j} \leq w^u_{4j}, \\ 0 \leq h^l_{wj} \leq h^u_{wj} \leq 1, \\ (j = 1, 2, \ldots, n), \end{cases} \tag{3}$$

where $R(\widetilde{w}_j)$ is the weight value of each expert, and $\widetilde{w}_B$ and $\widetilde{w}_w$ are those of the best and worst expert, respectively. The graded mean integration representation (GMIR) $R(\widetilde{w}_j)$ of the GITrFN $\widetilde{w}_j = [\widetilde{w}^l_j, \widetilde{w}^u_j]$ is defined as

$$R(\widetilde{w}_j) = \frac{1}{12}\left[(w^l_{1j} + 2w^l_{2j} + 2w^l_{3j} + w^l_{4j})h^l_{wj} \right.$$
$$\left. + (w^u_{1j} + 2w^u_{2j} + 2w^u_{3j} + w^u_{4j})h^u_{wj}\right]. \tag{4}$$

3. Risk-Assessment Process

The risk-assessment process is shown in Figure 1 and is as follows:

(1) The risk indicator system is established regarding 4M1E (man, machine, method, material, environment), and the work-breakdown-structure risk-breakdown-structure (WBS-RBS) method is used to prepare the risk list for the metro DFP.

(2) In determining the expert weights, the best expert and the worst expert are determined according to the expert weight index table. GITrF-BWM is used to analyze the weight of each expert, reduce the number

of pairwise comparisons, and improve the rationality of the expert-weight distribution.

(3) In terms of determining the weights of risk factors and evaluation indicators, each expert evaluates the relationship between each risk factor and each risk loss index in the form of scoring to form a pairwise judgment matrix. Herein, TL-ANP is used to calculate the weights of the four loss indicators and of each risk event so as to avoid the loss or distortion of evaluation information.

(4) The experts are then asked to rate the probability of the risk event and the four loss indicators after normalization. Compared to scoring only the probability of risk and economic loss, this method has a richer assessment content and can make a more refined assessment.

(5) Through the risk-identification framework, the event risk grade in the form of trapezoidal fuzzy numbers is converted into the belief structure of the impact of each risk event on the overall DFP risk and used as evidence of risk information fusion. After integrating the risk information, the most likely risk grade of the whole project is obtained.

4. Risk-Assessment Preparation

4.1. Expert Weights. Many experts with different backgrounds or fields are usually involved in risk assessment, and they have diverse professional grade, comprehensive ability, and familiarity with the assessed issues. We use these expert backgrounds as the basis for determining the best and worst experts, and we express the reference preferences of the best and worst experts in linguistic terms. The index scoring table for determining the expert weights is given in Table 2.

$$
\min \begin{pmatrix} \eta_{Bj}^{l+} + \eta_{Bj}^{l-} + \eta_{Bj}^{u+} + \eta_{Bj}^{u-} + \eta_{jW}^{l+} + \eta_{jW}^{l-} + \eta_{jW}^{u+} + \eta_{jW}^{u-} + \xi_{1Bj}^{l+} + \xi_{1Bj}^{l-} + \xi_{2Bj}^{l+} + \xi_{2Bj}^{l-} + \xi_{3Bj}^{l+} + \xi_{3Bj}^{l-} + \xi_{4Bj}^{l+} + \xi_{4Bj}^{l-} \\ + \xi_{1Bj}^{u+} + \xi_{1Bj}^{u-} + \xi_{2Bj}^{u+} + \xi_{2Bj}^{u-} + \xi_{3Bj}^{u+} + \xi_{3Bj}^{u-} + \xi_{4Bj}^{u+} + \xi_{4Bj}^{u-} + \xi_{1jW}^{l+} + \xi_{1jW}^{l-} + \xi_{2jW}^{l+} + \xi_{2jW}^{l-} + \xi_{3jW}^{l+} + \xi_{3jW}^{l-} + \xi_{4jW}^{l+} \\ + \xi_{4jW}^{l-} + \xi_{1jW}^{u+} + \xi_{1jW}^{u-} + \xi_{2jW}^{u+} + \xi_{2jW}^{u-} + \xi_{3jW}^{u+} + \xi_{3jW}^{u-} + \xi_{4jW}^{u+} + \xi_{4jW}^{u-} \end{pmatrix}
$$

$$
\text{s.t.} \begin{cases} \left(h_{wB}^l - h_{wj}^l \wedge h_{gBj}^l \right) - \eta_{Bj}^{l+} + \eta_{Bj}^{l-} = 0, \left(h_{wB}^u - h_{wj}^u \wedge h_{gBj}^u \right) - \eta_{Bj}^{u+} + \eta_{Bj}^{u-}, \\ \left(h_{wj}^l - h_{wj}^l \wedge h_{gBj}^l \right) - \eta_{Bj}^{l+} + \eta_{Bj}^{l-} = 0, \left(h_{wB}^u - h_{wj}^u \wedge h_{gBj}^u \right) - \eta_{Bj}^{u+} + \eta_{Bj}^{u-}, \\ \left(w_{1B}^l - w_{1j}^l g_{1Bj}^l \right) - \xi_{1Bj}^{l+} + \xi_{1Bj}^{l-} = 0, \left(w_{2B}^l - w_{2j}^l g_{2Bj}^l \right) - \xi_{2Bj}^{l+} + \xi_{2Bj}^{l-} = 0, \\ \left(w_{3B}^l - w_{3j}^l g_{3Bj}^l \right) - \xi_{3Bj}^{l+} + \xi_{3Bj}^{l-} = 0, \left(w_{4B}^l - w_{4j}^l g_{4Bj}^l \right) - \xi_{4Bj}^{l+} + \xi_{4Bj}^{l-} = 0, \\ \left(w_{1B}^u - w_{1j}^u g_{1Bj}^u \right) - \xi_{1Bj}^{u+} + \xi_{1Bj}^{u-} = 0, \left(w_{2B}^u - w_{2j}^u g_{2Bj}^u \right) - \xi_{2Bj}^{u+} + \xi_{2Bj}^{u-} = 0, \\ \left(w_{3B}^u - w_{3j}^u g_{3Bj}^u \right) - \xi_{3Bj}^{u+} + \xi_{3Bj}^{u-} = 0, \left(w_{4B}^u - w_{4j}^u g_{4Bj}^u \right) - \xi_{4Bj}^{u+} + \xi_{4Bj}^{u-} = 0, \\ \left(w_{1j}^l - g_{1jw}^l w_{1W}^l \right) - \xi_{1jw}^{l+} + \xi_{1jw}^{l-} = 0, \left(w_{2j}^l - g_{2jW}^l w_{2W}^l \right) - \xi_{2jw}^{l+} + \xi_{2jw}^{l-} = 0, \\ \left(w_{3j}^l - g_{3jW}^l w_{3W}^l \right) - \xi_{3jw}^{l+} + \xi_{3jw}^{l-} = 0, \left(w_{4j}^l - g_{4jW}^l w_{4W}^l \right) - \xi_{4jw}^{l+} + \xi_{4jw}^{l-} = 0, \\ \left(w_{1j}^u - g_{1jW}^u w_{1W}^u \right) - \xi_{1jw}^{u+} + \xi_{1jw}^{u-} = 0, \left(w_{2j}^u - g_{2jW}^u w_{2W}^u \right) - \xi_{2jw}^{u+} + \xi_{2jw}^{u-} = 0, \\ \left(w_{3j}^u - g_{3jW}^u w_{3W}^u \right) - \xi_{3jw}^{u+} + \xi_{3jw}^{u-} = 0, \left(w_{4j}^u - g_{4jW}^u w_{4W}^u \right) - \xi_{4jw}^{u+} + \xi_{4jw}^{u-} = 0, \\ w_{4i}^l + \sum_{j=1,l\neq i}^{n} w_{1j}^l \leq 1, w_{1i}^l + \sum_{j=1,l\neq i}^{n} w_{4j}^l \geq 1, w_{3i}^l + \sum_{j=1,l\neq i}^{n} w_{2j}^l \leq 1, w_{1i}^l \geq \sum_{j=1,l\neq i}^{n} w_{3i}^l (i=1,2,\ldots,n), \\ w_{4i}^u + \sum_{j=1,l\neq i}^{n} w_{1j}^u \leq 1, w_{1i}^u + \sum_{j=1,l\neq i}^{n} w_{4j}^u \geq 1, w_{3i}^u + \sum_{j=1,l\neq i}^{n} w_{2j}^u \leq 1, w_{1i}^u \geq \sum_{j=1,l\neq i}^{n} w_{3i}^u (i=1,2,\ldots,n), \\ w_{1j}^u \leq w_{1j}^l, w_{4j}^u \leq w_{4j}^l, 0 \leq h_{wi}^l \leq h_{wi}^u (i=1,2,\ldots,n), \\ 0 \leq w_{ki}^l \leq w_{(k+1)i}^l, 0 \leq w_{ki}^u \leq w_{(k+1)i}^u (i=1,2,\ldots,n), \\ \eta_{Bj}^{l+}\eta_{Bj}^{l-} = 0, \eta_{Bj}^{u+}\eta_{Bj}^{u-} = 0, \eta_{jW}^{l+}\eta_{jW}^{l-} = 0, \eta_{jW}^{u+}\eta_{jW}^{u-} = 0, \\ \xi_{1Bj}^{l+}\xi_{1Bj}^{l-} = 0, \xi_{2Bj}^{l+}\xi_{2Bj}^{l-} = 0, \xi_{3Bj}^{l+}\xi_{3Bj}^{l-} = 0, \xi_{4Bj}^{l+}\xi_{4Bj}^{l-} = 0, \\ \xi_{1Bj}^{u+}\xi_{1Bj}^{u-} = 0, \xi_{2Bj}^{u+}\xi_{2Bj}^{u-} = 0, \xi_{3Bj}^{u+}\xi_{3Bj}^{u-} = 0, \xi_{4Bj}^{u+}\xi_{4Bj}^{u-} = 0, \\ \xi_{1jW}^{l+}\xi_{1jW}^{l-} = 0, \xi_{2jW}^{l+}\xi_{2jW}^{l-} = 0, \xi_{3jW}^{l+}\xi_{3jW}^{l-} = 0, \xi_{4jW}^{l+}\xi_{4jW}^{l-} = 0, \\ \xi_{1jW}^{u+}\xi_{1jW}^{u-} = 0, \xi_{2jW}^{u+}\xi_{2jW}^{u-} = 0, \xi_{3jW}^{u+}\xi_{3jW}^{u-} = 0, \xi_{4jW}^{u+}\xi_{4jW}^{u-} = 0, \\ \eta_{Bj}^{l+} \geq 0, \eta_{Bj}^{l-} \geq 0, \eta_{Bj}^{u+} \geq 0, \eta_{Bj}^{u-} \geq 0, \eta_{jW}^{l+} \geq 0, \eta_{jW}^{l-} \geq 0, \eta_{jW}^{u+} \geq 0, \eta_{jW}^{u-} \geq 0, \\ \xi_{1Bj}^{u+} \geq 0, \xi_{1Bj}^{u-} \geq 0, \xi_{2Bj}^{u+} \geq 0, \xi_{2Bj}^{u-} \geq 0, \xi_{3Bj}^{u+} \geq 0, \xi_{3Bj}^{u-} \geq 0, \xi_{4Bj}^{u+} \geq 0, \xi_{4Bj}^{u-} \geq 0, \\ \xi_{1Bj}^{u+} \geq 0, \xi_{1Bj}^{u-} \geq 0, \xi_{2Bj}^{u+} \geq 0, \xi_{2Bj}^{u-} \geq 0, \xi_{3Bj}^{u+} \geq 0, \xi_{3Bj}^{u-} \geq 0, \xi_{4Bj}^{u+} \geq 0, \xi_{4Bj}^{u-} \geq 0, \\ \xi_{1jW}^{l+} \geq 0, \xi_{1jW}^{l-} \geq 0, \xi_{2jW}^{l+} \geq 0, \xi_{2jW}^{l-} \geq 0, \xi_{3jW}^{l+} \geq 0, \xi_{3jW}^{l-} \geq 0, \xi_{4jW}^{l+} \geq 0, \xi_{4jW}^{l-} \geq 0, \\ \xi_{1jW}^{u+} \geq 0, \xi_{1jW}^{u-} \geq 0, \xi_{2jW}^{u+} \geq 0, \xi_{2jW}^{u-} \geq 0, \xi_{3jW}^{u+} \geq 0, \xi_{3jW}^{u-} \geq 0, \xi_{4jW}^{u+} \geq 0, \xi_{4jW}^{u-} \geq 0, \\ (j=1,2,\ldots,n), \end{cases} \tag{5}
$$

where the positive-deviation variables and negative-deviation variables are expressed as follows:

$$\eta_{Bj}^{l+} = \left(h_{wB}^{l} - h_{wj}^{l} \wedge h_{gBj}^{l}\right) \vee 0,$$
$$\eta_{Bj}^{l-} = \left(h_{wj}^{l} \wedge h_{gBj}^{l} - h_{wB}^{l}\right) \vee 0,$$
$$\eta_{Bj}^{u+} = \left(h_{wB}^{u} - h_{wj}^{u} \wedge h_{gBj}^{u}\right) \vee 0,$$
$$\eta_{Bj}^{u-} = \left(h_{wj}^{u} \wedge h_{gBj}^{u} - h_{wB}^{u}\right) \vee 0,$$
$$\eta_{jW}^{l+} = \left(h_{wj}^{l} - h_{gjW}^{l} \wedge h_{wW}^{l}\right) \vee 0,$$
$$\eta_{Bj}^{l-} = \left(h_{gjW}^{l} \wedge h_{wW}^{l} - h_{wj}^{l}\right) \vee 0,$$
$$\eta_{jW}^{u+} = \left(h_{wj}^{u} - h_{gjW}^{u} \wedge h_{wW}^{u}\right) \vee 0,$$
$$\eta_{Bj}^{u-} = \left(h_{gjW}^{u} \wedge h_{wW}^{u} - h_{wj}^{u}\right) \vee 0,$$
$$\xi_{1Bj}^{l+} = \left(w_{1B}^{l} - w_{1j}^{l} g_{1Bj}^{l}\right) \vee 0,$$
$$\xi_{1Bj}^{l-} = \left(w_{1j}^{l} g_{1Bj}^{l} - w_{1B}^{l}\right) \vee 0,$$
$$\xi_{2Bj}^{l+} = \left(w_{2B}^{l} - w_{2j}^{l} g_{2Bj}^{l}\right) \vee 0,$$
$$\xi_{2Bj}^{l-} = \left(w_{2j}^{l} g_{2Bj}^{l} - w_{2B}^{l}\right) \vee 0,$$
$$\xi_{3Bj}^{l+} = \left(w_{3B}^{l} - w_{3j}^{l} g_{3Bj}^{l}\right) \vee 0,$$
$$\xi_{3Bj}^{l-} = \left(w_{3j}^{l} g_{3Bj}^{l} - w_{3B}^{l}\right) \vee 0,$$
$$\xi_{4Bj}^{l+} = \left(w_{4B}^{l} - w_{4j}^{l} g_{4Bj}^{l}\right) \vee 0,$$
$$\xi_{4Bj}^{l-} = \left(w_{4j}^{l} g_{4Bj}^{l} - w_{4B}^{l}\right) \vee 0,$$
$$\xi_{1Bj}^{u+} = \left(w_{1B}^{u} - w_{1j}^{u} g_{1Bj}^{u}\right) \vee 0,$$
$$\xi_{1Bj}^{u-} = \left(w_{1j}^{u} g_{1Bj}^{u} - w_{1B}^{u}\right) \vee 0,$$
$$\xi_{2Bj}^{u+} = \left(w_{2B}^{u} - w_{2j}^{u} g_{2Bj}^{u}\right) \vee 0,$$
$$\xi_{2Bj}^{u-} = \left(w_{2j}^{u} g_{2Bj}^{u} - w_{2B}^{u}\right) \vee 0, \qquad (6)$$
$$\xi_{3Bj}^{u+} = \left(w_{3B}^{u} - w_{3j}^{u} g_{3Bj}^{u}\right) \vee 0,$$
$$\xi_{3Bj}^{u-} = \left(w_{3j}^{u} g_{3Bj}^{u} - w_{3B}^{u}\right) \vee 0,$$
$$\xi_{4Bj}^{u+} = \left(w_{4B}^{u} - w_{4j}^{u} g_{4Bj}^{u}\right) \vee 0,$$
$$\xi_{4Bj}^{u-} = \left(w_{4j}^{u} g_{4Bj}^{u} - w_{4B}^{u}\right) \vee 0,$$
$$\xi_{1jW}^{l+} = \left(w_{1j}^{l} - w_{1W}^{l} g_{1jW}^{l}\right) \vee 0,$$
$$\xi_{1jW}^{l-} = \left(w_{1W}^{l} g_{1jW}^{l} - w_{1j}^{l}\right) \vee 0,$$
$$\xi_{2jW}^{l+} = \left(w_{2j}^{l} - w_{2W}^{l} g_{2jW}^{l}\right) \vee 0,$$
$$\xi_{2jW}^{l-} = \left(w_{2W}^{l} g_{2jW}^{l} - w_{2j}^{l}\right) \vee 0,$$
$$\xi_{3jW}^{l+} = \left(w_{3j}^{l} - w_{3W}^{l} g_{3jW}^{l}\right) \vee 0,$$
$$\xi_{3jW}^{l-} = \left(w_{3W}^{l} g_{3jW}^{l} - w_{3j}^{l}\right) \vee 0,$$
$$\xi_{4jW}^{l+} = \left(w_{4j}^{l} - w_{4W}^{l} g_{4jW}^{l}\right) \vee 0,$$
$$\xi_{4jW}^{l-} = \left(w_{4W}^{l} g_{4jW}^{l} - w_{4j}^{l}\right) \vee 0,$$
$$\xi_{1jW}^{u+} = \left(w_{1j}^{u} - w_{1W}^{u} g_{1jW}^{u}\right) \vee 0,$$
$$\xi_{1jW}^{u-} = \left(w_{1W}^{u} g_{1jW}^{u} - w_{1j}^{u}\right) \vee 0,$$
$$\xi_{2jW}^{u+} = \left(w_{2j}^{u} - w_{2W}^{u} g_{2jW}^{u}\right) \vee 0,$$
$$\xi_{2jW}^{u-} = \left(w_{2W}^{u} g_{2jW}^{u} - w_{2j}^{u}\right) \vee 0,$$
$$\xi_{3jW}^{u+} = \left(w_{3j}^{u} - w_{3W}^{u} g_{3jW}^{u}\right) \vee 0,$$
$$\xi_{3jW}^{u-} = \left(w_{3W}^{u} g_{3jW}^{u} - w_{3j}^{u}\right) \vee 0,$$
$$\xi_{4jW}^{u+} = \left(w_{4j}^{u} - w_{4W}^{u} g_{4jW}^{u}\right) \vee 0,$$
$$\xi_{4jW}^{u-} = \left(w_{4W}^{u} g_{4jW}^{u} - w_{4j}^{u}\right) \vee 0,$$

where the symbol $\vee$ is the maximum operator and the symbol $\wedge$ is the minimum operator.

Herein, fuzzy numbers are used to represent the comparative relationship among experts. However, the traditional fuzzy numbers used directly to deal with uncertain information have certain limitations because (i) the same fuzzy language level has different meanings to different people and (ii) the membership function of traditional fuzzy numbers is an accurate function and so is inappropriate for describing imprecise sensory information. Therefore, herein GITrF-BWM is used to determine the expert GITrF weights.

To solve equation (3), some positive-deviation variables and negative-deviation variables are introduced, and a programming model such as equation (5) is established. After solving equation (5), the optimal GITrF weight vector can be obtained. It is noted that equation (5) is a goal programming model because there are only some positive-deviation variables and negative-deviation variables in the objective function, and it can be solved using the LINGO 11 software.

4.2. Obtaining the Risk Grade of a Risk Event. In risk-control systems, WBS-RBS is commonly used for risk identification. After identifying all the risk events related to the construction of a metro DFP, the risks are categorized upward layer by layer until the total target of the system to establish the risk indicator system for metro DFP construction.

According to the risk-assessment method provided variously in the literature [25–27], the risk value is usually expressed as $R_l = P_l * C_l \, (l = 1, \ldots L)$. After identifying all possible risks with WBS-RBS, risk categorization is carried out to establish a risk evaluation indicator system for metro DFP construction, and then the probability of each construction risk event and four loss indicators are evaluated in the system. The probability of occurrence and all types of losses can be divided into five grades. The loss is subdivided into direct economic loss, construction delay loss, casualties loss, and surrounding environmental impact loss. The classification criteria of these probabilities and various losses can be set according to the suggestions in the aforementioned guide, and the membership function corresponding to each grade can be obtained, as given in Tables 3 and 4.

Considering the weight of each expert's score, m experts evaluate the occurrence probability of the lth risk and the four losses. The membership function of each risk loss is normalized by minimum-maximum normalization, and the membership functions derived from the evaluation of different loss indicators are converted to the range of [0, 1] by linearization. Taking the economic loss as an example, the normalization equation is

$$c_{l,e}^{i*} = \frac{c_{l,e}^{i} - c_{l,e,\max}^{i}}{c_{l,e,\max}^{i} - c_{l,e,\min}^{i}}, \qquad (7)$$

where $c_{l,e,max}^{i}$ is $c_{l,e,d}^{i}$ in the membership function, and $c_{l,e,\min}^{i}$ is $c_{l,e,a}^{i}$ in the membership function; the same pertains to the construction delay, environmental impact, and human casualties, and the results are given in Table 5. After normalization, each risk-loss evaluation is fused according to the weight of each risk indicator, and the final membership functions of risk occurrence probability and loss are

TABLE 1: The corresponding GITrFNs and the expert score difference of the linguistic terms for the GITrF-BWM.

| Linguistic terms	GITrFNs	Overall score difference of experts
Equally important (EI)	[(1.000, 1.000, 1.000, 1.000; 1.000), (1.000, 1.000, 1.000, 1.000; 1.000)]	(0, 5)
Weakly important (WI)	[(0.782, 1.019, 1.154, 1.379; 0.800), (0.664, 0.899, 1.257, 1.500; 1.000)]	(5, 10)
Fairly important (FI)	[(1.648, 1.934, 2.075, 2.360; 0.800), (1.500, 1.789, 2.218, 2.500; 1.000)]	(10, 15)
Very important (VI)	[(2.647, 2.934, 3.076, 3.361; 0.800), (2.500, 2.790, 3.218, 3.500; 1.000)]	(15, 20)
Absolutely important (AI)	[(3.653, 3.938, 4.078, 4.363; 0.800), (3.500, 3.793, 4.222, 4.500; 1.000)]	(20, 25)
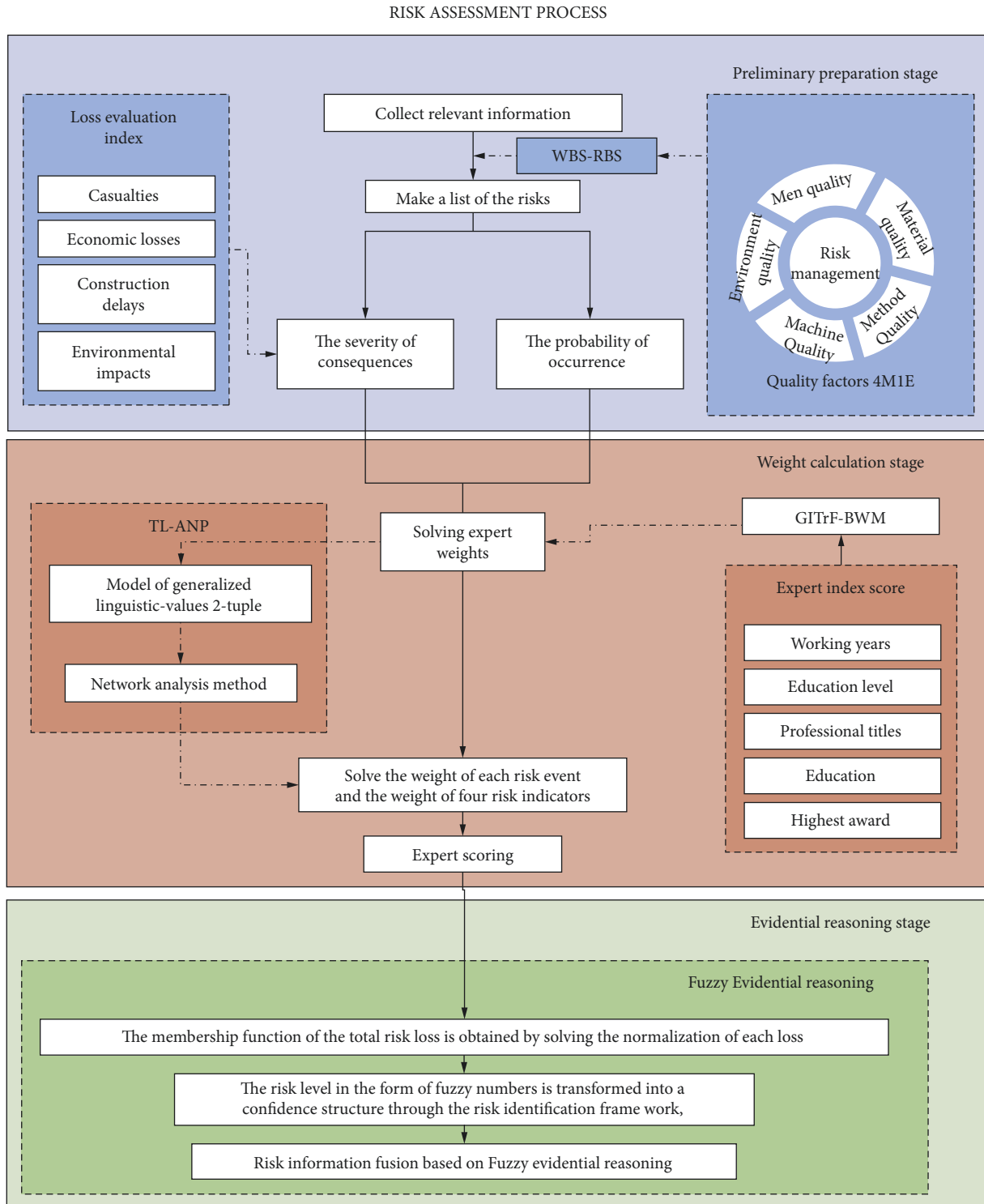
FIGURE 1: Flowchart of risk assessment.

TABLE 2: Expert weight indicator table.

Indicators	Indicator grade				
Length of service	0–5	5–10	10–15	15–20	≥20
Record of formal schooling	Specialized subject	Undergraduate course	Master's degree	Doctor	Postdoctoral
The title	Other	Primary	Intermediate	Deputy senior	Senior
The winning	Other	Municipal	Provincial	National	World
Score	1	2	3	4	5

TABLE 3: Corresponding relation between risk occurrence probability grade standard and membership function.

Grade	Language assessment	Probability interval	Membership function
1	Impossibility	$P \leq 0.01\%$	{0, 0, 0.00005, 0.0001}
2	Infrequent	$0.01\% \leq P \leq 0.1\%$	{0.00005, 0.0001, 0.001, 0.0055}
3	Occasionally	$0.1\% \leq P \leq 1\%$	{0.00055, 0.001, 0.01, 0.055}
4	Possible	$1\% \leq P \leq 10\%$	{0.0055, 0.01, 0.1, 0.55}
5	Frequently	$P \geq 10\%$	{0.055, 0.1, 1, 1}

TABLE 4: Corresponding relation between risk loss grade standard and membership function (1).

Grade	Language assessment	Economic losses	Delay time	Environmental impact	Casualties
1	Ignored	C1 ≤ 500	C2 ≤ 1	C3 ≤ 50	C4 ≤ 5
2	Considered	500 ≤ C1 ≤ 1000	1 ≤ C2 ≤ 3	50 ≤ C3 ≤ 100	5 ≤ C4 ≤ 10
3	Serious	1000 ≤ C1 ≤ 5000	3 ≤ C2 ≤ 6	100 ≤ C3 ≤ 500	10 ≤ C4 ≤ 50
4	Very serious	5000 ≤ C1 ≤ 10000	6 ≤ C2 ≤ 12	500 ≤ C3 ≤ 1000	50 ≤ C4 ≤ 100
5	Catastrophic	C1 ≥ 10000	C2 ≥ 12	C3 ≥ 1000	C4 ≥ 100
Corresponding relation between risk loss grade standard and membership function (2)					
1	Ignored	{0, 0, 250, 500}	{0, 0, 1, 2}	{0, 0, 25, 50}	{0, 0, 2, 5}
2	Considered	{250, 500, 1000, 3000}	{1, 1, 3, 5}	{25, 50, 100, 300}	{2, 5, 10, 30}
3	Serious	{750, 1000, 5000, 7500}	{2, 3, 6, 9}	{75, 100, 500, 750}	{8, 10, 50, 75}
4	Very serious	{3000, 5000, 10000, 55000}	{4, 6, 12, 18}	{300, 500, 1000, 5500}	{30, 50, 100, 550}
5	Catastrophic	{7500, 10000, 100000, 100000}	{9, 12, 24, 24}	{750, 1000, 10000, 10000}	{75, 100, 1000, 1000}

TABLE 5: Relationship between risk loss grade and membership function after normalization.

Grade	Economic losses	Delay time	Environmental impact	Casualties
1	{0, 0, 0.0025, 0.005}	{0, 0, 0.04, 0.08}	{0, 0, 0.0025, 0.005}	{0, 0, 0.002, 0.005}
2	{0.0025, 0.005, 0.01, 0.03}	{0.04, 0.04, 0.12, 0.21}	{0.0025, 0.005, 0.01, 0.03}	{0.002, 0.005, 0.01, 0.03}
3	{0.0075, 0.01, 0.05, 0.075}	{0.08, 0.13, 0.25, 0.38}	{0.0075, 0.01, 0.05, 0.075}	{0.008, 0.01, 0.05, 0.075}
4	{0.03, 0.05, 0.1, 0.55}	{0.17, 0.25, 0.5, 0.75}	{0.03, 0.05, 0.1, 0.55}	{0.03, 0.05, 0.10, 0.55}
5	{0.075, 0.1, 1, 1}	{0.375, 0.5, 1, 1}	{0.075, 0.1, 1, 1}	{0.075, 0.1, 1, 1}

$$P_l = \left\{ \frac{\sum_{i=1}^{m} \omega^i \times p_{l,a}^i}{\sum_{i=1}^{m} \omega^i}, \frac{\sum_{i=1}^{m} \omega^i \times p_{l,b}^i}{\sum_{i=1}^{m} \omega^i}, \frac{\sum_{i=1}^{m} \omega^i \times p_{l,c}^i}{\sum_{i=1}^{m} \omega^i}, \frac{\sum_{i=1}^{m} \omega^i \times p_{l,d}^i}{\sum_{i=1}^{m} \omega^k} \right\},$$

(8)

$$c_l = \left\{ \frac{\sum_{i=1}^{m} \omega^i \times c_{l,a}^i}{\sum_{i=1}^{m} \omega^i}, \frac{\sum_{i=1}^{m} \omega^i \times c_{l,b}^i}{\sum_{i=1}^{m} \omega^i}, \frac{\sum_{i=1}^{m} \omega^i \times c_{l,c}^i}{\sum_{i=1}^{m} \omega^i}, \frac{\sum_{i=1}^{m} \omega^i \times c_{l,d}^i}{\sum_{i=1}^{m} \omega^i} \right\},$$

(9)

where $c_{l,a}^i$, $c_{l,b}^i$, $c_{l,c}^i$, and $c_{l,d}^i$ are the evaluation results of the fusion of the four normalized risk losses by experts. The expert weights are then fused to form a membership function for the total risk loss of each risk event.

After obtaining the probabilities of risk events and the total risk loss, the risk-identification framework is established according to

$$R_k = \{R_{ka}, R_{kb}, R_{kc}, R_{kd}\}$$

$$= \{\min\left([P_{lia} \otimes C_{sia}]\right),$$

$$\frac{\left[\sum_{li=1}^{p} \sum_{si=1}^{c} P_{lib} \otimes C_{sib}\right]}{[p \times c]}, \frac{\left[\sum_{li=1}^{p} \sum_{si=1}^{c} P_{lic} \otimes C_{sic}\right]}{[p \times c]},$$

(10)

$$\max\left([P_{lid} \otimes C_{sid}]\right)\},$$

where "[ ]" means that only the effective combination, that is, a certain grade of risk membership function needs to consider the combination of probability and consequences, need to see the risk evaluation matrix on the guide to assess, called the effective combination, the risk evaluation matrix in the risk guide is given in Table 6. Suppose that H_n denotes risk grade n, which can be obtained by combining p sets of probabilities and c sets of losses, where $n = 1, 2 \ldots 5$, $1 \le p \le 5$ and $1 \le c \le 5$.

4.3. Determining Weights of Risks and Loss Indicators.
After Sections 4.1 and 4.2, the relationship between the grade of a single risk event and the membership function can be obtained. To further obtain the overall risk level of the metro DFP, classical ANP was extended by using linguistic variables instead of the values on a scale of 1–9 (Table 7), and TL-ANP was proposed for the analytical calculation of risk weights and indicator weights. TL-ANP determines the weights of not only individual risk factors but also loss indicators. Herein, the steps of TL-ANP are illustrated by the example of determining the weights of each risk.

Step 1: Establish the network structure

The risk factors are u_{jk}, and a set of them is U_j ($j = 1, 2, \ldots, 12$). Based on the 12 risk-factor sets of (i) pit precipitation, (ii) maintenance structure, (iii) foundation treatment, (iv) pit excavation, (v) main structure, (vi) surrounding buildings, (vii) expansive rock, (viii) carbonaceous mudstone, (ix) fill, (x) earthquake, (xi) surrounding pipelines, and (xii) windstorm and the interactions among the risk factors under them, a network structure is constructed

Step 2: Determine the weight matrix A

Construct a judgment matrix $A^i = (a^i_{kj})_{n \times n}$ ($i = 1, 2, \ldots n$) for each set of risk factors based on the linguistic two-tuple values. Here, $w_i = (w_{i1}, w_{i2}, \ldots w_{in})^T$ is the weight vector of matrix A^i ($i = 1, 2, \ldots n$), which can be obtained using equation (11). Integrating w_i ($n = 1, 2.., n$) gives the weight matrix A:

$$w_{ik} = \Delta\left(\frac{\sum_{j=1}^{n} \Delta^{-1}(a^i_{kj})}{\sum_{k=1}^{n} \sum_{j=1}^{n} \Delta^{-1}(a^i_{kj})}\right) (i, k = 1, 2, \ldots, n), \tag{11}$$

$$A = \begin{pmatrix} a_{11} & \cdots & \cdots & a_{112} \\ \vdots & \ddots & & \vdots \\ \vdots & & \ddots & \vdots \\ a_{121} & \cdots & \cdots & a_{1212} \end{pmatrix}. \tag{12}$$

Step 3: Determine the supermatrix

Similar to the method for determining A, the matrix W_{ij} ($i, j = 1, 2, \ldots, n$) is obtained by comparing the interactions between the risk factors u_{ik} in the risk-factor set U_i and those in the other risk-factor sets, whereupon the final super matrix W is formed.

Step 4: Calculate the weighted supermatrix $\overline{W}$

TABLE 6: Risk evaluation matrix.

Risk	Risk of loss				
	Ignore	Consider	Serious	Very serious	Disaster
$P \le 0.01\%$	1	1	2	3	4
$0.01\% \le P \le 0.1\%$	1	2	3	3	4
$0.1\% \le P \le 1\%$	1	2	3	4	5
$1\% \le P \le 10\%$	2	3	4	4	5
$P \ge 10\%$	2	3	4	5	5

TABLE 7: Linguistic terms corresponding to linguistic variables for pairwise comparisons.

Linguistic variable	Linguistic terms
Extreme weak	S0
Extreme weak	S2
Weak	S3
Moderately weak	S4
Equally strong	S5
Moderately strong	S6
Strong	S7
Very strong	S8
Extremely strong	S9

This is done as

$$\overline{W} = \Delta\left(\Delta^{-1}(A) \times \Delta^{-1}(W)\right). \tag{13}$$

Step 5: Calculate the limit matrix W^{∞} and obtain the weights of risk factors $\omega = (\omega_1, \omega_2, \ldots, \omega_t)^T$

This is done as

$$W^{\infty} = \Delta\left(\lim_{k \to \infty} \left(\Delta^{-1}(\overline{W})\right)^k\right). \tag{14}$$

5. Risk-Assessment Model for a Metro Deep Foundation Pit

5.1. Transformation of Indicator Risk Belief Structure.
The risk level of each event contributes to the overall risk grade of the metro DFP construction. FER involves quantifying the impact of each risk event on the overall risk grade rating, i.e., the risk level of each risk event is used as the evidence that the overall project is rated as having a specific risk grade, and all the evidence is aggregated at the end. The belief structure of the event risk level is transformed as follows:

(1) Draw the membership function curve of metro DFP construction risk grade, i.e., the membership function curve of risk-identification framework $H = \{H_n, n = 1, 2, \ldots 5\}$, and plot the membership function curve of the risk level R_l for each risk event l.

(2) Find the intersection area of the membership function of risk level R_l of each event l and the membership function of each level H_n in the risk-identification framework, which is the membership degree of risk event l to the overall risk being rated H_n. Finally, the above-obtained degree of the membership function is normalized to obtain the
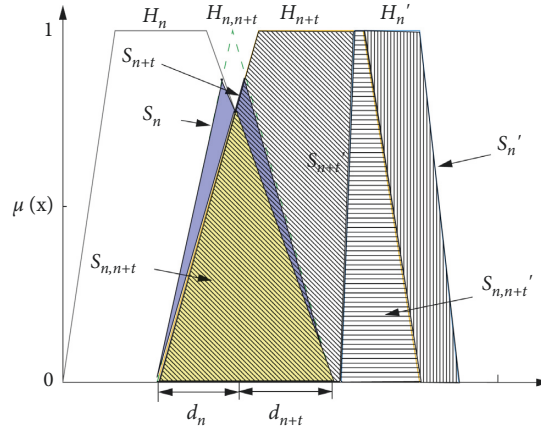
Figure 2: Intersection of different fuzzy grades.

Table 8: Formulas related to belief redistribution.

	The intersection of two fuzzy evaluation grades is less than 1	The intersection of the two fuzzy evaluation grades is equal to 1
The magnitude of redistribution to β_n	$\beta_n^{n,(n+t)} = (s_n + AF_n^{n,(n+t)} \cdot s_{n,(n+t)}/s_n + s_{n,(n+t)} + s_{(n+t)})\beta_{n,(n+t)}$	$\beta_n^{n,(n+t)} = AF_n^{n,(n+t)}\beta_{n,(n+t)}$
The magnitude of redistribution to β_{n+t}	$\beta_{n+t}^{n,(n+t)} = (AF_n^{n,(n+t)} \cdot s_{n,(n+t)} + s_{n+1}/s_n + s_{n,(n+t)} + s_{(n+t)})\beta_{n,(n+t)}$	$\beta_{n+t}^{n,(n+t)} = AF_{n+t}^{n,(n+t)}\beta_{n,(n+t)}$
Distribution coefficient of β_n	$AF_n^{n,(n+t)} = (1/2)[(1 - (d_n/d_n + d_{n+t})) + (S_n/S_n + S_{n+t})]$	$AF_n^{n,(n+t)} = 1 - (S_n' + S_{n,(n+t)}'/S_n' + 2S_{n,(n+t)}' + S_{n+t}')$
Distribution coefficient of β_{n+t}	$AF_n^{n,(n+t)} = (1/2)[(1 - (d_{n+t}/d_n + d_{n+t})) + (S_{n+t}/S_n + S_{n+t})]$	$AF_n^{n,(n+t)} = 1 - (S_{n,(n+t)}' + S_{n+t}'/S_n' + 2S_{n,(n+t)}' + S_{n+t}')$

belief structure $\gamma_n^l (n = 1, 2, \ldots 5)$ of each event risk grade in the risk-identification framework.

5.2. Risk Information Fusion Based on Evidential Reasoning.
In Sections 4.3 and 5.1, each risk event's weight and belief structure are obtained, respectively, and the FER algorithm is used for evidence fusion [8, 28] to obtain the overall risk grade of metro DFP construction. First, we calculate the basic belief σ_n^l of each risk event:

$$\sigma_n^l = \eta_l \gamma_n^l, \tag{15}$$

$$\sigma_H^l = 1 - \sum_{n=1}^{5} \sigma_n^l, \tag{16}$$

where σ_n^l is the basic belief in risk event l having risk grade H_n, and σ_H^l is the risk that cannot be determined because of lack of information:

$$\overline{\sigma}_H^l = 1 - \eta_l,$$
$$\overline{\sigma}_H = k\left[\prod_{l=1}^{L} \overline{\sigma}_H^l\right]. \tag{17}$$

The FER algorithm is used to fuse the information of risk factors to obtain the risk-evaluation results of the metro DFP, and the specific algorithm is as follows:

$$\sigma_n = k\left\{\prod_{l=1}^{L}[\sigma_n^l + \sigma_H^l] - \prod_{l=1}^{L}\sigma_H^l\right\}, \quad n = 1, 2, \ldots 5, \tag{18}$$

$$\sigma_{n,(n+t)} = k\mu_{Fn,(n+t)}^{\max}\left\{\prod_{l=1}^{L}[\sigma_n^l + \sigma_{n+t}^l + \sigma_H^l] - \prod_{l=1}^{L}[\sigma_n^l + \sigma_H^l]\right.$$
$$\left. - \prod_{l=1}^{L}[\sigma_{n+t}^l + \sigma_H^l] + \prod_{l=1}^{L}\sigma_H^l\right\}, \quad n = 1, 2, \ldots 5, \tag{19}$$
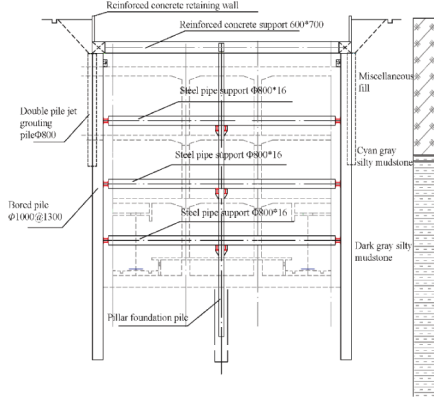
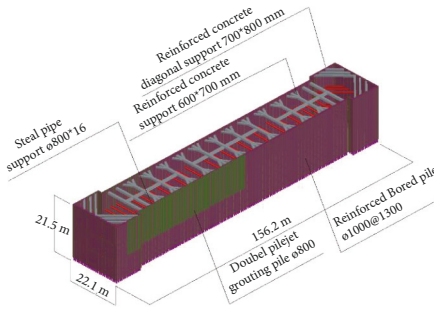Figure 3: Cross section of the foundation pit.
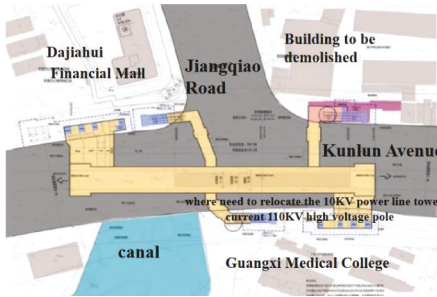

Figure 4: Schematic diagram of foundation pit support.

Figure 5: General layout of Jiangqiao station.

Table 9: Linguistic fuzzy reference comparisons between criteria.

Expert	E1	E2	E3	E4	E5	E6	E7	E8	E9	E10
Best expert E3	FI	WI	EI	FI	VI	AI	WI	WI	FI	AI
Worst expert E6	FI	VI	AI	WI	WI	EI	VI	VI	FI	EI

$$
k = \left\{
\begin{array}{c}
\sum_{n=1}^{5} \left\{ \prod_{l=1}^{L} \left[\sigma_n^l + \sigma_H^l\right] - \prod_{j=1}^{L} \sigma_H^l \right\} \\
+ \sum_{t=1}^{4} \sum_{n=1}^{5-t} \mu_{H_{n,(n+1)}}^{\max} \left\{ \prod_{l=1}^{L} \left[\sigma_n^l + \sigma_{n+t}^l + \sigma_H^l\right] - \prod_{l=1}^{L} \left[\sigma_{n+t}^l + \sigma_H^l\right] \right\} \\
+ \prod_{l=1}^{L} \sigma_H^l \right\} + \prod_{l=1}^{L} \sigma_H^l
\end{array}
\right\}^{-1},
$$

(20)

$$
\beta_n = \frac{\sigma_n}{1 - \overline{\sigma}_H},
$$

(21)

$$
\beta_{n,(n+t)} = \frac{\sigma_{n,n+1}}{1 - \overline{\sigma}_H}.
$$

(22)

First, the fusion equations (18)–(20) are used to obtain the mass functions σ_n and $\sigma_{n,n+t}$ of the basic belief of the DFP risk evaluation on H_n and $H_{n,(n+t)}$, where $H_{n,(n+t)}$ is the intersection of fuzzy grades H_n and $H_{(n+t)}$. k is the normalized coefficient, and the final evaluation result is obtained using equations (21) and (22). β_n is the belief that the overall pit risk is evaluated to grade H_n after combining the L risk factors, $\beta_{n,n+1}$ is the belief about the fuzzy risk grade $H_{n,(n+t)}$, and the fuzzy intersection belief $\beta_{n,n+1}$ should be redistributed to β_n and β_{n+t}.

Because there are different cases of intersection of H_n and $H_{(n+t)}$, the way to redistribute $\beta_{n,n+1}$ is different, and the intersection of different cases is shown in Figure 2. Suppose that the maximum affiliation of the intersection of two fuzzy grades is less than one, as shown in Figure 2. $\beta_{n,n+1}$ can be redistributed according to Table 8, and $\beta_n^{n,(n+t)}$ and $\beta_{n+t}^{n,(n+t)}$ represent the allocated values $\beta_{n,n+1}$. If the maximum membership degree of the intersection of the two fuzzy evaluation grades is equal to one, as shown in Figure 2, then s_n and s_{n+t} become zero. Table 8 The specific equations are given in Table 8.

Finally, $\beta_{n,(n+1)} = (n = 1, 2, \ldots 4, t = 1, 2, \ldots 4, n + t \le 5)$ are redistributed to β_n and β_{n+t}, and the distributed belief is superimposed on the belief obtained from equation (21) to obtain the final β_n.

6. Case Analysis

6.1. Project Overview. As part of the phase-I project of Line 5 of Nanning Metro, Jiangqiao Metro Station is located at the intersection of Kunlun Avenue and Jiangqiao Road. The total length of the station is 156.2 m, its width is 22.1 m, and its floor depth is 21.5–23.6 m. Jiangqiao station is an underground three-island platform station, and its construction method is cut and cover. The construction pit support is made from bored piles with internal support, and a water curtain made of 800-mm-diameter rotary piles is used to hold back the water in the thick fill layer near the culvert at the station's western end. Figure 3 shows the DFP in cross section, and Figure 4 shows its support schematically. Seven dewatering wells are arranged in the main part of the station, and four are set in the auxiliary structure. To the northeast of the station are houses built by the villagers of Jiangqiao Village, and to the northwest is the Dajiahui commercial office building. There are high-voltage cable towers to the south of the station, and the surrounding military optical cables and power pipelines are complicated. The general layout of the Jiangqiao station is shown in Figure 5.

6.2. Data Acquisition. Ten experts were invited to evaluate the construction of the DFP project. The best expert E_3 and the worst expert E_6 were selected by a priori scoring based on each

TABLE 10: Expert index score.

Expert	Working years	Educational background	Job title	Top prize	Score	Score difference	GMIR
1	3	3	3	1	10	3	0.0905
2	3	4	3	4	14	5	0.1012
3	5	4	4	4	17	EB	0.1374
4	1	3	3	2	9	6	0.0972
5	2	2	2	2	8	4	0.0867
6	2	2	1	1	6	EW	0.0740
7	4	3	4	3	14	5	0.1146
8	3	3	3	3	12	5	0.1273
9	3	3	3	2	11	4	0.0933
10	2	2	1	1	6	6	0.0779

expert's background, and the linguistic reference preferences of the best and worst experts were provided (see Table 9). Then, GITr-BWM was applied to calculate the weights of each expert. From Tables 1 and 9, the GITrF best-expert-to-other-experts and other-experts-to-worst-expert vectors are obtained:

$$\widetilde{G}_B = [\widetilde{g}_{B1}, \widetilde{g}_{B2}, \widetilde{g}_{B3}, \widetilde{g}_{B4}, \widetilde{g}_{B5}, \widetilde{g}_{B6}, \widetilde{g}_{B7}, \widetilde{g}_{B8}, \widetilde{g}_{B9}, \widetilde{g}_{B10}],$$
$$\widetilde{G}_W = [\widetilde{g}_{1W}, \widetilde{g}_{2W}, \widetilde{g}_{3W}, \widetilde{g}_{4W}, \widetilde{g}_{5W}, \widetilde{g}_{6W}, \widetilde{g}_{7W}, \widetilde{g}_{8W}, \widetilde{g}_{9W}, \widetilde{g}_{10W}],$$
(23)

where

$$\widetilde{g}_{B1} = [(1.648, 1.934, 2.075, 2.360; 0.800), (1.500, 1.789, 2.218, 2.500; 1.000)],$$
$$\widetilde{g}_{B2} = [(0.782, 1.019, 1.154, 1.379; 0.800), (0.664, 0.899, 1.257, 1.500; 1.000)],$$
$$\widetilde{g}_{B10} = [(3.653, 3.938, 4.078, 4.363; 0.800), (3.500, 3.793, 4.222, 4.500; 1.000)],$$
$$\widetilde{g}_{1W} = [(1.648, 1.934, 2.075, 2.360; 0.800), (1.500, 1.789, 2.218, 2.500; 1.000)],$$
$$\widetilde{g}_{2W} = [(2.647, 2.934, 3.076, 3.361; 0.800), (2.500, 2.790, 3.218, 3.500; 1.000)],$$
$$\widetilde{g}_{10W} = [(1.000, 1.000, 1.000, 1.000; 1.000), (1.000, 1.000, 1.000, 1.000; 1.000)].$$
(24)

From equation (5), a goal programming model was established, and after solving it using LINGO 11, we obtained the optimal GITrF weight vector for the experts: $w^* = [w_1^*, w_2^*, w_3^*, w_4^*, w_5^*, w_6^*, w_7^*, w_8^*, w_9^*, w_{10}^*]$, where

$$w_1^* = [(0.482, 0.698, 0.954, 1.198; 0.08), (0.209, 0.397, 0.608, 1.400; 0.19)],$$
$$w_2^* = [(0.495, 0.700, 1.000, 1.250; 0.11), (0.141, 0.285, 0.800, 1.500; 0.17)],$$
$$w_3^* = [(0.530, 0.780, 1.050, 1.272; 0.125), (0.125, 0.350, 0.800, 1.600; 0.240)],$$
$$w_{10}^* = [(0.521, 0.764, 0.987, 1.208; 0.10), (0.124, 0.251, 0.700, 1.400; 0.12)].$$
(25)

Calculating their GMIRS, the result is shown in Table 10, these being the weights of the experts.

Based on the structure system of DFP-construction risk evaluation, after several rounds of screening, we finally obtained 30 construction risk factors, as shown in Figure 6. The 10 experts had to conduct two evaluations. The first evaluation involved each expert using TL-ANP to evaluate the importance of the 30 risk events just obtained. The purpose was to use TL-ANP to obtain the weight of each risk event and loss index. The DFP risk network relationship is shown in Figure 7, where the results of one of the experts' judgments are used as an example to illustrate the TL-ANP. Based on Step 2 in Section 4.3, the decision maker describes the factors in each risk-factor set using binary semantics according to the criteria in Table 7, and the weight matrix A

of the 12 risk-factor sets is derived after the operations in Step 2, as given in Table 11. The supermatrix W for each risk factor can be obtained in a similar way, as given in Table 12. The linguistic two-tuple values are transformed using equation (2), and the limit supermatrix $\overline{W}$ is obtained using equation (15). The limit matrix W^∞ is equivalent to $(\Delta^{-1}(\overline{W}))^{30}$, from which it can be seen that the weights of the risk factors are $\omega_1 = (s_0, 0.0300)$, $\omega_2 = (s_0, 0.0214)$, $\omega_3 = (s_0, 0.0234)$, $\omega_4 = (s_0, 0.0210), \ldots \omega_{29} = (s_0, 0.0312)$, $\omega_{30} = (s_0, 0.0334)$. According to formula (2), the expert's evaluation results of the risk factor weight can be obtained: $\omega_1 = 0.030$, $\omega_2 = 0.021$, $\omega_3 = 0.023$, $\omega_4 = 0.021, \ldots \omega_{29} = 0.031$, $\omega_{30} = 0.033$.

Based on the weights of the 10 experts, the TL-ANP evaluation results of each expert on the weights of the risk
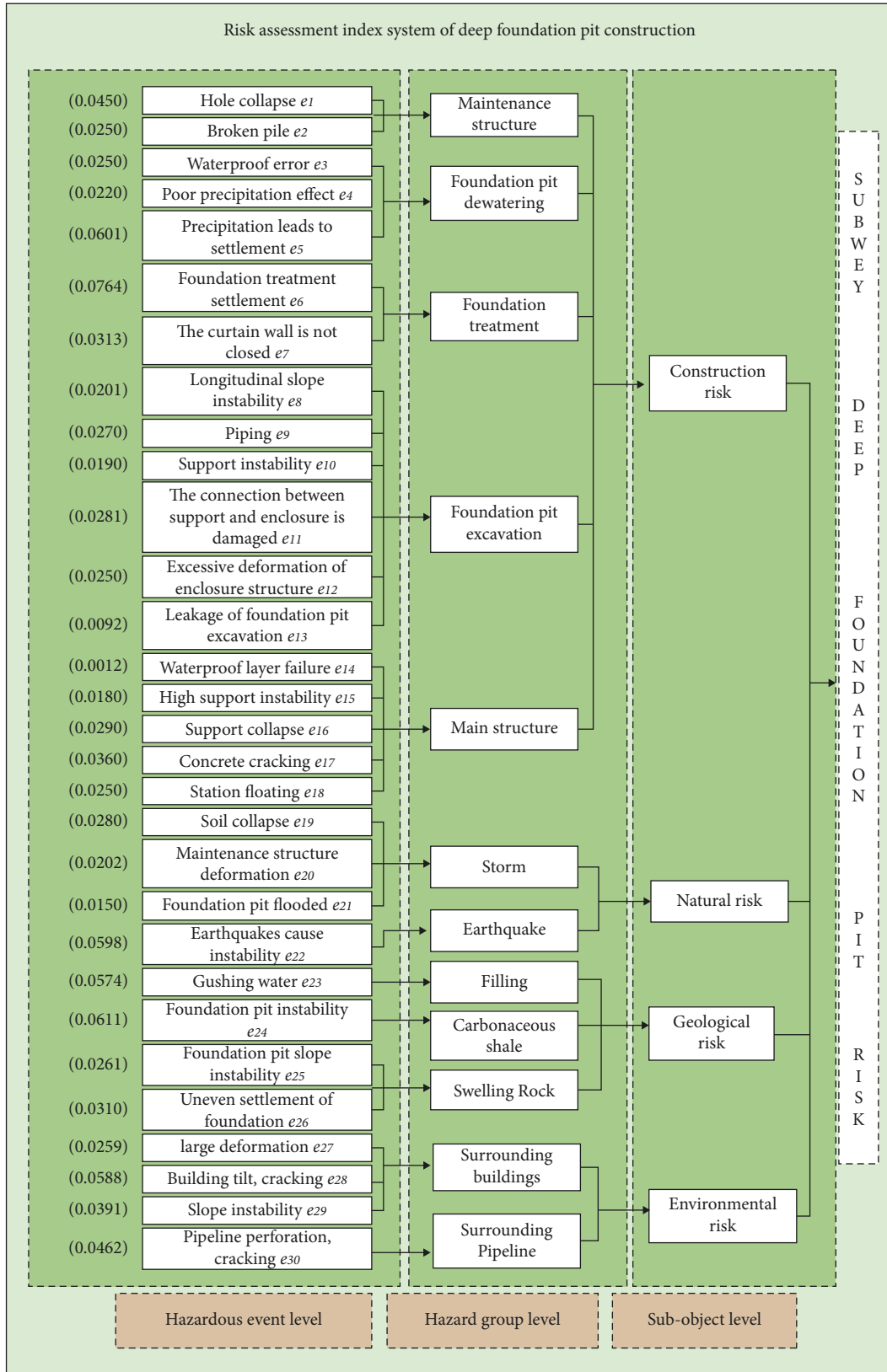
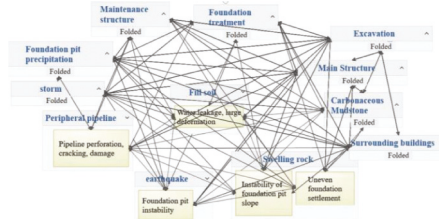FIGURE 6: Risk system of DFP construction.

Figure 7: Network relationship diagram of metro deep foundation pit risk events.

Table 11: Weight matrix.

	U1	U2	U3	U4	U5	U6	U7	U8	U9	U10	U11	U12
U1	(S1, −0.046)	(S0, 0)	(S1, −0.045)	(S0, 0.012)	(S1, −0.019)	(S1, 0.012)	(S1, 0.024)	(S1, −0.029)	(S1, 0.024)	(S0, 0)	(S1, −0.024)	(S1, −0.025)
U2	(S0, 0.048)	(S1, 0.012)	(S1, 0.032)	(S1, 0.013)	(S0, 0.039)	(S1, 0.012)	(S1, −0.022)	(S1, 0.039)	(S0, 0.043)	(S1, −0.032)	(S0, 0.038)	(S1, 0.058)
U3	(S1, 0.038)	(S1, 0.038)	(S0, 0.012)	(S1, 0.048)	(S1, −0.022)	(S1, −0.038)	(S0, 0)	(S1, −0.024)	(S1, −0.047)	(S1, 0.012)	(S1, −0.022)	(S0, 0.017)
U4	(S1, 0.026)	(S1, 0.056)	(S0, 0.026)	(S0, 0.056)	(S0, 0.037)	(S0, 0.047)	(S1, 0.058)	(S0, 0.037)	(S0, 0.031)	(S1, 0.059)	(S1, 0.027)	(S0, 0.030)
U5	(S1, −0.026)	(S0, 0)	S1, 0.026)	(S1, −0.023)	(S1, 0.021)	(S1, −0.025)	(S1, 0.039)	(S0, 0.044)	(S1, −0.013)	(S0, 0)	(S0, 0.031)	(S0, 0.026)
U6	(S1, −0.041)	(S1, 0.012)	(S1, 0.014)	(S0, 0.012)	(S0, 0.048)	(S1, −0.023)	(S1, −0.014)	(S1, −0.048)	(S0, 0.012)	(S1, −0.014)	(S0, 0.048)	(S1, −0.026)
U7	(S1, −0.033)	(S0, 0)	(S0, 0.014)	(S1, −0.023)	(S1, −0.042)	(S1, −0.042)	(S1, 0.023)	(S0, 0.022)	(S1, −0.023)	(S1, 0.030)	(S1, −0.038)	(S1, −0.035)
U8	(S0, 0.021)	(S1, −0.054)	(S1, −0.054)	(S1, −0.054)	(S1, −0.043)	(S1, −0.055)	(S1, −0.055)	(S1, −0.043)	(S1, −0.054)	(S1, 0.026)	(S1, −0.043)	(S1, −0.033)
U9	(S0, 0.021)	(S0, 0)	(S0, 0.012)	(S0, 0.013)	(S0, 0.027)	(S0, 0.037)	(S0, 0)	(S1, 0.047)	(S0, 0.023)	(S0, 0)	(S0, 0.027)	(S1, 0.021)
U10	(S1, −0.026)	(S1, −0.054)	(S1, −0.044)	(S1, −0.044)	(S1, −0.017)	(S0, 0.044)	(S1, −0.054)	(S0, 0.012)	(S1, −0.015)	(S1, −0.054)	(S1, −0.017)	(S0, 0.011)
U11	(S0, 0.039)	(S1, −0.050)	(S1, −0.040)	(S1, −0.051)	(S1, −0.015)	(S0, 0.048)	(S0, 0)	(S1, −0.045)	(S1, −0.021)	(S1, −0.026)	(S1, −0.015)	(S1, −0.017)
U12	(S1, −0.024)	(S1, 0.038)	(S1, 0.044)	(S1, 0.039)	(S1, −0.014)	(S1, −0.018)	(S0, 0)	(S1, −0.013)	(S1, 0.038)	(S0, 0)	(S1, −0.013)	(S1, −0.027)

Table 12: Supermatrix.

	u1	u2	u3	u4	...	u27	u28	u29	u30
u1	(S4, −0.0625)	(S4, 0)	(S5, 0)	(S0, 0)	...	(S5, 0)	(S0, 0)	(S0, 0)	(S3, −0.0625)
u2	(S5, −0.0625)	(S4, 0)	(S3, 0)	(S0, 0)	...	(S3, 0)	(S0, 0)	(S0, 0)	(S6, −0.0625)
u3	(S1, 0.0417)	(S4, −0.0278)	(S3, 0.0139)	(S2, 0.0278)	...	(S4, −0.0278)	(S2, − 0.0417)	(S3, −0.0556)	(S3, −0.0556)
u4	(S3, 0.0139)	(S2, −0.0556)	(S2, −0.0278)	(S2, −0.0556)	...	(S1, −0.0556)	(S4, −0.0278)	(S1, 0.0556)	(S2, − 0.0139)
...	...	...	...	...	...	...	...	...	...
u27	(S2, −0.0278)	(S3, −0.0556)	(S4, −0.0417)	(S3, 0.0417)	...	(S3, 0.0139)	(S3, 0.0556)	(S0, 0)	(S2, −0.0278)
u28	(S3, −0.0556)	(S4, −0.0278)	(S1, 0)	(S2, 0.0139)	...	(S2, −0.0278)	(S3, 0.0556)	(S4, −0.0278)	(S3, −0.0556)
u29	(S4, −0.0556)	(S2, −0.0278)	(S3, 0)	(S2, −0.0278)	...	(S2, −0.0278)	(S3, −0.0278)	(S2, −0.0278)	(S4, −0.0417)
u30	(S2, −0.0139)	(S2, 0.0556)	(S4, 0)	(S4, 0.0139)	...	(S4, 0.0556)	(S2, −0.0278)	(S2, 0.0556)	(S2, −0.0278)

factors were assembled, and the combined weight size of each risk factor was obtained as $\omega = (0.045, 0.025, 0.025, 0.020, 0.060, 0.076, 0.031, 0.020, 0.027, 0.019, 0.028, 0.025, 0.009, 0.012, 0.018, 0.029, 0.036, 0.025, 0.020, 0.015, 0.060, 0.057, 0.061, 0.026, 0.031, 0.026, 0.059, 0.039, 0.046)^T$ (as given in Table 13).

The risk event weights are attached to the DFP-construction risk evaluation system, as shown in Figure 6. Also,

using the same method, the weights of the four losses of economic loss, delay time, environmental impact, and casualties are 0.574, 0.148, 0.139, and 0.139, respectively.

The second assessment was that each expert evaluated independently the possibility of each event and the degree of each loss indicator. The evaluation results were normalized using equation (7) and combined with the loss indicator weights to obtain the overall loss affiliation function. Then,

TABLE 13: Evaluation results of risk factor weight by experts.

	ωE1	ωE2	ωE3	ωE4	ωE5	ωE6	ωE7	ωE8	ωE9	ωE10	ω
u1	0.030	0.024	0.031	0.032	0.032	0.063	0.059	0.058	0.064	0.057	0.045
u2	0.021	0.019	0.020	0.023	0.024	0.024	0.026	0.029	0.031	0.029	0.025
u3	0.023	0.028	0.023	0.020	0.022	0.022	0.026	0.027	0.029	0.028	0.025
u4	0.021	0.022	0.021	0.019	0.023	0.019	0.019	0.020	0.019	0.019	0.020
u5	0.070	0.067	0.070	0.073	0.069	0.049	0.048	0.051	0.052	0.051	0.060
u6	0.081	0.075	0.082	0.078	0.083	0.063	0.070	0.078	0.070	0.080	0.076
u7	0.025	0.021	0.023	0.023	0.029	0.039	0.038	0.040	0.039	0.030	0.031
u8	0.021	0.023	0.027	0.014	0.020	0.019	0.019	0.019	0.019	0.018	0.020
u9	0.032	0.031	0.035	0.033	0.032	0.022	0.022	0.020	0.025	0.011	0.027
u10	0.028	0.022	0.024	0.027	0.028	0.013	0.013	0.014	0.013	0.007	0.019
u11	0.028	0.027	0.023	0.022	0.028	0.033	0.029	0.035	0.028	0.028	0.028
u12	0.020	0.017	0.024	0.021	0.022	0.029	0.035	0.031	0.029	0.021	0.025
u13	0.011	0.010	0.013	0.010	0.015	0.007	0.006	0.007	0.006	0.006	0.009
u14	0.015	0.016	0.016	0.011	0.016	0.010	0.009	0.008	0.008	0.008	0.012
u15	0.021	0.022	0.020	0.020	0.021	0.018	0.015	0.014	0.018	0.015	0.018
u16	0.020	0.020	0.022	0.023	0.022	0.036	0.040	0.035	0.040	0.033	0.029
u17	0.033	0.040	0.031	0.036	0.032	0.040	0.039	0.041	0.036	0.033	0.036
u18	0.027	0.030	0.023	0.031	0.026	0.022	0.022	0.022	0.024	0.023	0.025
u19	0.031	0.031	0.033	0.030	0.033	0.029	0.028	0.021	0.020	0.030	0.028
u20	0.022	0.020	0.020	0.022	0.023	0.021	0.020	0.018	0.017	0.023	0.020
u21	0.013	0.012	0.012	0.014	0.013	0.019	0.015	0.017	0.015	0.020	0.015
u22	0.063	0.072	0.069	0.062	0.063	0.057	0.053	0.052	0.054	0.057	0.060
u23	0.066	0.068	0.063	0.068	0.068	0.048	0.046	0.048	0.052	0.053	0.057
u24	0.063	0.065	0.069	0.070	0.062	0.055	0.055	0.052	0.057	0.060	0.061
u25	0.026	0.022	0.026	0.023	0.028	0.028	0.027	0.028	0.028	0.027	0.026
u26	0.032	0.030	0.032	0.032	0.033	0.031	0.032	0.032	0.031	0.030	0.031
u27	0.029	0.029	0.032	0.023	0.020	0.026	0.024	0.023	0.025	0.027	0.026
u28	0.063	0.054	0.060	0.068	0.061	0.061	0.057	0.052	0.052	0.060	0.059
u29	0.031	0.035	0.025	0.034	0.022	0.049	0.049	0.047	0.049	0.049	0.039
u30	0.033	0.044	0.029	0.034	0.029	0.048	0.062	0.064	0.053	0.069	0.046

the probability and loss evaluations of all the experts were combined using equation (8) and equation (9). The risk grade for each risk event was calculated by multiplying the probability of the event and the loss, as given in Table 14.

6.3. Risk Assessment.

The risk-identification framework was constructed according to the method introduced in Section 4.2. Equation (10) was used to work out the corresponding relationship between risk grade standard and membership function, as given in Table 15. The risk grade membership function of metro DFP construction risk events was then transformed into a belief structure through the risk-identification framework, and the basic belief distribution function σ_n^l and unallocated belief σ_H^l of each risk event l were calculated according to equation (15) and equation (16), as given in Table 16.

By fusing equations (18)–(20), we obtain the basic belief σ_n for the overall risk of the Jiangqiao station rated as grade H_n, and the basic belief $\sigma_{n,(n+t)}$ for the intersection grade $H_{n,n+t}$, as given in Table 17. We then use equations (21) and (22) to obtain the belief value β_n of the overall risk grades and the belief $\beta_{n,(n+t)}$ value of the intersection of the grades, as given in Table 18. According to the different fuzzy risk grade intersection cases, the fuzzy intersection belief is distributed by Table 8. The belief distribution coefficient and the distribution results are given in Tables 19 and 20,

respectively. Finally, the distributed belief is superimposed on the nonintersection belief to obtain the final belief of the DFP being rated at each level, as given in Table 21. The final results show that the most likely overall metro DFP risk is the second-grade risk with a probability of 0.2479. As Table 15 shows, the metro DFP with this risk level must be strengthened for daily management scrutiny.

7. Discussion

7.1. Analysis of Results.

The overall risk grade has been derived, but which risk events and risk loss indicators should be focused on in risk control requires further analysis. To clarify the key factors affecting the risk of this project and the critical loss indicators, the following four aspects are analyzed.

(1) Each risk event weight is kept constant, the belief structure is changed by changing the event risk level in the same type, and the impact of each event risk level change on the overall risk level is compared. Here, the belief β_2^l of each risk event in the risk-identification framework is set to zero in turn, and the risk grade belonging to the overall risk is calculated based on this. The comparison results are presented in Figure 8, which shows that the risk factors that have more impact on the evaluation of

Table 14: List of possibility, loss, and risk grade of all risk events in metro deep foundation pit.

Risk events	Probability	Loss	Grade of risk
Hole collapse (e_1)	(0.01, 0.017, 0.175, 0.182)	(0.029, 0.040, 0.120, 0.222)	(2.81E − 04, 7.07E − 04, 0.021, 0.041)
Broken pile (e_2)	(0.006, 0.008, 0.084, 0.095)	(0.022, 0.033, 0.071, 0.162)	(1.2E − 04, 2.74 E − 04, 0.006, 0.015)
Waterproof failures (e_3)	(3.2E − 05, 6.6E − 05, 0.001, 0.004)	(0.017, 0.024, 0.057, 0.131)	(5.5E − 07, 1.5E − 06, 3.8E − 05, 4.7E − 04)
Poor precipitation effect (e_4)	(0.001, 0.001, 0.010, 0.054)	(0.015, 0.022, 0.072, 0.112)	(8.0E − 06, 2.1E − 05, 7.0 E − 04, 0.006)
Precipitation induced settlement (e_5)	(0.001, 0.001, 0.012, 0.063)	(0.025, 0.035, 0.098, 0.157)	(1.5E − 05, 4.2E − 05, 0.001, 0.010)
Settlement caused by foundation treatment (e_6)	(1E − 04, 2.5E − 04, 0.003, 0.014)	(0.014, 0.0197, 0.054, 0.111)	(2.0E − 06, 5.0E − 06, 1.42 E − 04, 0.002)
Curtain wall not enclosed (e_7)	(8.3E − 05, 1.6E − 04, 0.002, 0087)	(0.011, 0.014, 0.040, 0.072)	(8.9E − 07, 2.2E − 06, 6.3E − 05, 6.3E − 04)
Longitudinal slope instability (e_8)	(3.9E − 05, 7.7E − 05, 7.8E − 04, 0.004)	(0.020, 0.030, 0.073, 0.167)	(7.9E − 07, 2.3E − 06, 5.7E − 05, 7.0E − 04)
Piping (e_9)	(1.7E − 04, 3.2E − 04, 0.003, 0.018)	(0.020, 0.029, 0.088, 0.158)	(3.6E − 06, 9.5E − 06, 2.9 E − 04, 0.003)
Support loss of stability (e_{10})	(7.6E − 05, 1.4E − 04, 0.015, 0.008)	(0.029, 0.040, 0.114, 0.206)	(2.2E − 06, 5.8E − 06, 1.65 E − 04, 0.002)
Support connection damaged (e_{11})	(9.0E − 05, 1.7E − 04, 0.002, 0.010)	(0.034, 0.047, 0.157, 0.241)	(3.0E − 06, 7.9E − 06, 2.6E − 04, 2.2E − 03)
Surrounding deformation is too large	(0.006, 0.010, 0.095, 0.106)	(0.030, 0.040, 0.145, 0.192)	(1.7E − 04, 3.8E − 04, 0.014, 0.020)
The excavation caused water leakage	(5.4E − 04, 8.9E − 04, 0.010, 0.054)	(0.018, 0.025, 0.062, 0.129)	(9.7E − 06, 2.3E − 05, 6.0E − 04, 0.007)
Waterproof layer failure (e_{14})	(8.1E − 05, 1.5E − 04, 0.0013, 0.008)	(0.019, 0.027, 0.065, 0.114)	(1.5E − 06, 4.2E − 06, 8.7E − 05, 9.4E − 04)
Failure of high support (e_{15})	(2.3E − 04, 4.2E − 04, 0.004, 0.024)	(0.032, 0.047, 0.105, 0.205)	(7.3E − 06, 2.0E − 05, 4.2E − 04, 0.005)
Support collapsed (e_{16})	(5.9E − 04, 0.001, 0.011, 0.059)	(0.040, 0.057, 0.209, 0.257)	(2.4E − 05, 6.2E − 05, 0.002, 0.015)
Concrete cracking (e_{17})	(9.1E − 05, 1.7E − 04, 0.002, 0.010)	(0.025, 0.038, 0.086, 0.186)	(2.3E − 06, 6.6 E − 06, 2E − 04, 0.002)
The station floats as a whole (e_{18})	(6.3E − 04, 0.001, 0.012, 0.065)	(0.012, 0.018, 0.081, 0.176)	(7.4E − 06, 2.1E − 05, 9.3E − 04, 0.012)
The earthwork collapsed (e_{19})	(5.8E − 04, 0.001, 0.011, 0.059)	(0.029, 0.044, 0.098, 0.257)	(1.7E − 05, 4.6E − 05, 0.001, 0.015)
Maintenance structure deformation	(8.7E − 05, 1.6E − 04, 0.002, 0.009)	(0.016, 0.023, 0.061, 0.101)	(1.4E − 06, 3.8E − 06, 1E − 04, 9.3E − 04)
Foundation pit flooded (e_{21})	(1E − 04, 2.7E − 04, 0.003, 0.015)	(0.020, 0.027, 0.066, 0.138)	(2.9E − 06, 7.3E − 06, 1.8E − 04, 0.002)
Earthquake instability (e_{22})	(0.005, 0.009, 0.094, 0.115)	(0.060, 0.084, 0.336, 0.446)	(3.1E − 04, 7.9E − 04, 0.032, 0.051)
Well-up water (e_{23})	(5.3E − 04, 0.001, 0.009, 0.049)	(0.018, 0.025, 0.062, 0.101)	(9.6E − 06, 2.5E − 05, 5.9E − 04, 0.005)
Foundation pit instability (e_{24})	(9.0E − 05, 1.7E − 04, 0.002, 0.010)	(0.026, 0.040, 0.089 0.199)	(2.4E − 06, 6.7E − 06, 1.3E − 04, 0.002)
Foundation pit slope instability (e_{25})	(9.1E − 05, 1.7E − 04, 0.002, 0.010)	(0.021, 0.029, 0.070, 0.138)	(1.9E − 06, 5E − 06, 1.2E − 04, 0.001)
Uneven settlement of foundation (e_{26})	(1E − 04, 2E − 04, 0.002, 0.012)	(0.017, 0.023, 0.059, 0.128)	(1.8E − 06, 4.6E − 06, 1.1E − 04, 0.002)
Water leakage, large deformation (e_{27})	(8.4E − 05, 1.7E − 04, 0.002, 0.008)	(0.022, 0.033, 0.077, 0.179)	(1.9E − 06, 5.2E − 06, 1.3E − 04, 0.001)
Inclining cracking of building (e_{28})	(7.7E − 05, 1.4E − 04, 0.001, 0.008)	(0.028, 0.042, 0.093, 0.238)	(2.2E − 06, 6.1E − 06, 1.2E − 04, 0.002)
Slope instability (e_{29})	(3.5E − 05, 6.9E − 05, 7.1E − 04, 0.004)	(0.028, 0.040, 0.088, 0.213)	(9.8E − 07, 2.7E − 06, 6.2E − 05, 8.4E − 04)
Pipeline perforation cracking (e_{30})	(4.5E − 05, 9.1E − 05. 9.1E − 04, 0.005)	(0.018, 0.025, 0.066, 0.115)	(8.0E − 07, 2.3E − 06, 5.8E − 05, 5.6E − 04)

TABLE 15: Corresponding relation between risk grade standard and membership function (Risk Identification Framework).

Grade	Language assessment	Control scheme	Membership function
1	Ignored	Daily management and review	{0, 0, 0.00002, 0.00086}
2	Permissible	Strengthen daily management review	{0, 0.000002, 0.001772, 0.01572}
3	Acceptable	Monitoring measures are needed	{0, 0.000189, 0.004886834, 0.05571}
4	Unacceptable	Establish control and warning measures	{0, 0.001501, 0.01746, 0.31792}
5	Refuse to accept	Stop immediately and rectify	{0.0000648, 0.006323275, 0.5457625, 1}

TABLE 16: Belief distribution function list of all risk events in metro deep foundation pit construction.

Risk events	Basic belief distribution function					
	σ_1^l	σ_2^l	σ_3^l	σ_4^l	σ_5^l	σ_H^l
Hole collapse (e_1)	0.0069	0.0173	0.0138	0.0069	0.0017	0.9533
Broken pile (e_2)	0.0011	0.0088	0.0088	0.0062	0.0035	0.9715
Waterproof failures (e_3)	0.0052	0.0074	0.0066	0.0058	0.0016	0.9734
Poor precipitation effect (e_4)	0.0049	0.0054	0.0045	0.0052	0.0022	0.9778
Precipitation induced settlement (e_5)	0.0187	0.0187	0.0202	0.0025	0.0013	0.9386
Settlement caused by foundation treatment (e_6)	0.0407	0.0238	0.0068	0.0051	0.0041	0.9195
Curtain wall not enclosed (e_7)	0.0049	0.0061	0.0110	0.0094	0.0033	0.9654
Longitudinal slope instability (e_8)	0.0062	0.0077	0.0046	0.0015	0.0005	0.9794
Piping (e_9)	0.0068	0.0077	0.0087	0.0039	0.0019	0.9711
Support loss of stability (e_{10})	0.0038	0.0086	0.0038	0.0029	0.0010	0.9801
Support connection damaged (e_{11})	0.0054	0.0080	0.0094	0.0054	0.0007	0.9712
Surrounding deformation is too large	0.0000	0.0138	0.0080	0.0032	0.0016	0.9734
The excavation caused water leakage	0.0015	0.0025	0.0037	0.0015	0.0005	0.9903
Waterproof layer failure (e_{14})	0.0010	0.0040	0.0037	0.0033	0.0018	0.9862
Failure of high support (e_{15})	0.0053	0.0075	0.0030	0.0023	0.0008	0.9813
Support collapsed (e_{16})	0.0071	0.0095	0.0067	0.0057	0.0019	0.9691
Concrete cracking (e_{17})	0.0081	0.0100	0.0093	0.0085	0.0048	0.9592
The station floats as a whole (e_{18})	0.0055	0.0078	0.0070	0.0047	0.0016	0.9734
The earthwork collapsed (e_{19})	0.0070	0.0062	0.0070	0.0078	0.0054	0.9666
Maintenance structure deformation	0.0025	0.0064	0.0059	0.0052	0.0022	0.9778
Foundation pit flooded (e_{21})	0.0018	0.0024	0.0056	0.0051	0.0025	0.9825
Earthquake instability (e_{22})	0.0000	0.0070	0.0352	0.0176	0.0070	0.9332
Well-up water (e_{23})	0.0010	0.0013	0.0549	0.0002	0.0001	0.9425
Foundation pit instability (e_{24})	0.0087	0.0185	0.0179	0.0161	0.0083	0.9306
Foundation pit slope instability (e_{25})	0.0024	0.0049	0.0122	0.0065	0.0008	0.9731
Uneven settlement of foundation (e_{26})	0.0073	0.0104	0.0077	0.0056	0.0043	0.9647
Water leakage, large deformation (e_{27})	0.0040	0.0080	0.0073	0.0066	0.0032	0.9709
Inclining cracking of building (e_{28})	0.0127	0.0145	0.0165	0.0151	0.0076	0.9336
Slope instability (e_{29})	0.0109	0.0109	0.0090	0.0083	0.0028	0.9581
Pipeline perforation cracking (e_{30})	0.0013	0.0051	0.0144	0.0253	0.0087	0.9451

TABLE 17: Basic belief of risk information fusion and intersection.

n	σ_n	$\sigma_{1,n}$	$\sigma_{2,n}$	$\sigma_{3,n}$	$\sigma_{4,n}$
1	0.0883				
2	0.1081	0.0232			
3	0.1007	0.0183	0.0271		
4	0.0936	0.0151	0.0245	0.0237	
5	0.0543	0.0008	0.0117	0.0130	0.0124

TABLE 18: Overall belief values of risk information fusion at all risk grades and the belief values at the intersection of risk grades.

n	β_n	$\beta_{1,n}$	$\beta_{2,n}$	$\beta_{3,n}$	$\beta_{4,n}$
1	0.14352				
2	0.17579	0.03770			
3	0.16381	0.02980	0.04390		
4	0.15219	0.02450	0.03981	0.03859	
5	0.08829	0.00137	0.01904	0.02111	0.02016

foundation construction risk are (i) excessive surface deformation caused by foundation treatment (e_6), (ii) tilting and cracking of surrounding buildings (e_{28}), and (iii) welling-up water (e_{23}), with (i) being the most influential factor. Its changes impact the belief of each risk grade by 11.95%, −34.60%, 8.49%, 10.42%, and 17.94%, respectively. The risk events with greater weights also have more

impact on the overall risk evaluation, and the above three risk events are precisely the three with high-risk weight, which coincides with our subjective intuition. The reason for this result is that each risk event's weight must be considered in the risk fusion calculation process. It is verified that the fuzzy evidence inference method considers the risk level

Table 19: Belief distribution coefficient of each intersection belief.

n	$AF_1^{1,n}$: $AF_n^{1,n}$	$AF_2^{2,n}$: $AF_n^{2,n}$	$AF_3^{3,n}$: $AF_n^{3,n}$	$AF_4^{4,n}$: $AF_n^{4,n}$
2	0.53 : 0.47			
3	0.87 : 0.13	0.53 : 0.47		
4	0.23 : 0.77	0.49 : 0.51	0.55 : 0.45	
5	0.45 : 0.55	0.61 : 0.39	0.40 : 0.60	0.39 : 0.61

Table 20: Results of distribution grade intersection belief to each grade.

n	β_1	β_2	β_3	β_4	β_5
β_1		0.019981	0.025926	0.005635	0.000617
β_2	0.017719		0.023267	0.019507	0.011614
β_3	0.003874	0.020633		0.021225	0.008444
β_4	0.018865	0.020303	0.017366		0.007862
β_5	0.000754	0.007426	0.012666	0.012298	

Table 21: Belief of overall risk of deep foundation pit of Jianqiao Station.

	β_1	β_2	β_3	β_4	β_5
Basic beliefs	0.14352	0.17579	0.16381	0.15219	0.08829
Distribution beliefs	0.05216	0.07211	0.05418	0.06439	0.03314
Total beliefs	0.19568	0.24790	0.21797	0.21657	0.12143
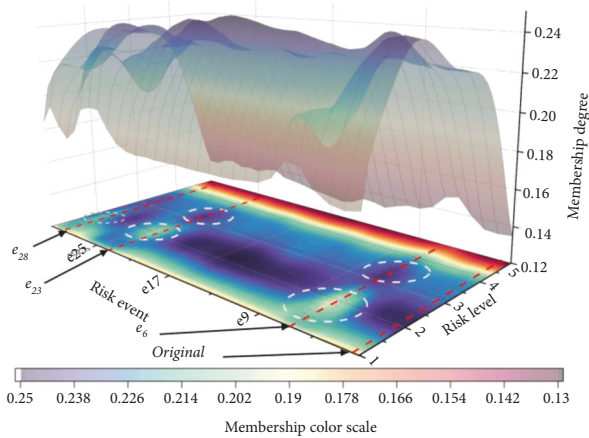
Figure 8: Influence of risk level changes of different events on the overall risk grade of foundation pit.
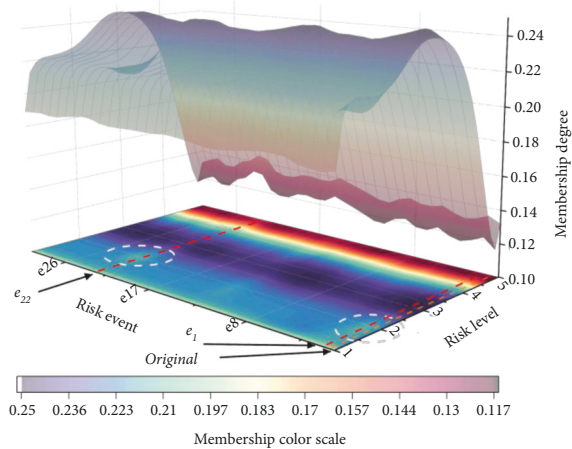
Figure 9: Influence of risk level changes of different events on the overall risk grade of foundation pit under the same weight.
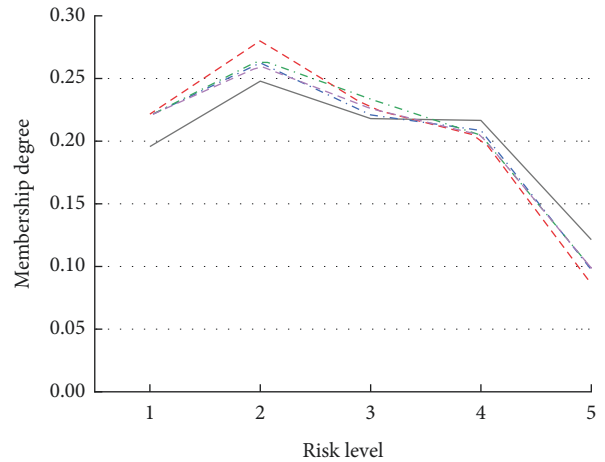
Figure 10: Effect of changes in the level of each loss indicator on the overall risk level in the case of consideration of loss indicator weights in uneven settlement of the foundation.

of each risk event as the evidence reflecting the risk level of DFP construction, which reflects the importance of risk event weights to fuzzy evidence inference.

(2) Without considering the influence of each risk event weight, at this stage, the FER algorithm gives the belief of risk grade evaluation of Nanning Jianqiao station with equal weights as $\beta_k = [(H_1, 0.1857), (H_2, 0.2218), (H_3, 0.2487), (H_4, 0.2021), (H_5, 0.1417)]$. Similarly, we change the belief β_2^l of risk events (set to zero in turn) and compare the effect of
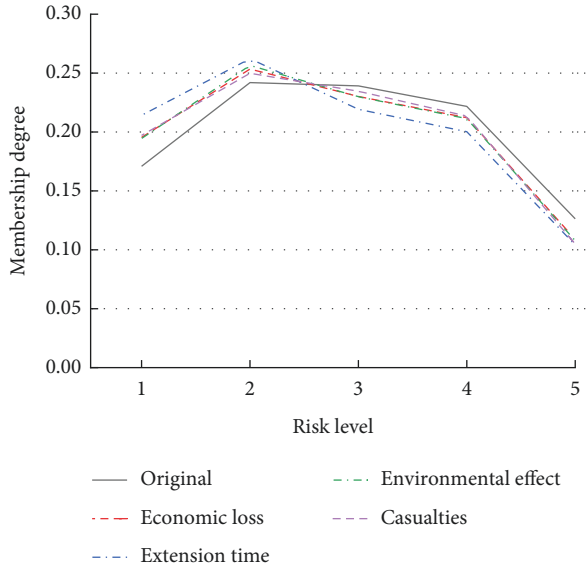
FIGURE 11: Effect of changes in the level of each loss indicator on the overall risk level without considering the weight of loss indicators in the case of uneven settlement of the foundation.
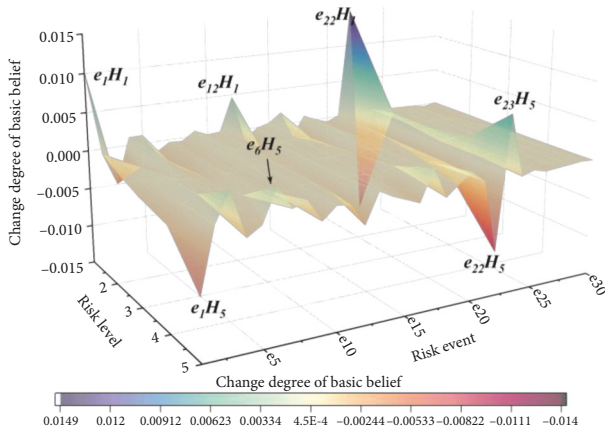

FIGURE 12: Changes of basic belief of each risk event on the overall risk before and after considering the weight of loss indicator.
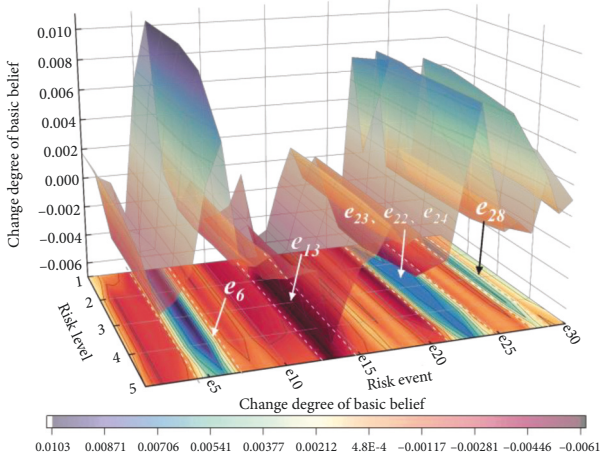

FIGURE 13: Changes in the basic belief of each risk event to the overall risk before and after considering the weight of risk events.

different event belief structure changes on the evaluation of the overall risk grade of the DFP. The comparison results are shown in Figure 9. The risk events with the most impact on the risk grade of DFP construction are hole collapse of the enclosure structure (e_1) and earthquake-induced DFP instability (e_{22}). These risk events have the common feature that their basic belief σ_n^l is distributed unevenly; there are obvious peaks and valleys, and these risk events also deserve to be alerted. However, compared with the case of considering the weights of risk events, when the weights are not considered, then the degree of risk evaluation is affected less, and it is a risk event of secondary focus.

(3) The weights of each loss evaluation indicator remain unchanged, and the membership functions of all loss evaluation indicators of a certain risk event are changed in the same way in turn. We compare the impact of the change in the evaluation level of different loss indicators on the overall risk grade of the DFP. Here, the membership functions of the losses caused by uneven foundation settlement (e_{26}) are selected and set to {0, 0, 0, 0} in turn. The comparison results are presented in Figure 10, which shows that the risk loss indicator with the greatest impact on DFP-construction risk grade is economic loss. According to the equation $R = P \times C$ for risk in the Risk Management Guide for Metro and Underground Construction [1], the loss grade directly affects the risk grade, and the greater the weight of the loss indicator, the greater the impact on the risk grade, so it can also affect the results of the final evidence fusion. As the loss indicator with the largest weight, the economic loss has the greatest impact on the overall risk-assessment results, which is a reasonable explanation. Subject to the mutual restraint of various losses, compared with the impact of risk event weight, the loss indicator has less impact on the evaluation of the whole risk grade, indicating that the subdivision of loss indicators is better for avoiding evaluation abnormalities.

(4) Regardless of the influences of the weights of the loss evaluation indicators, those weights are set to be equal. The FER algorithm gives the project risk evaluation indicators' combined belief as $\beta_k = [(H_1, 0.1677), (H_2, 0.2408), (H_3, 0.2379), (H_4, 0.2292), (H_5, 0.1249)]$. We set the membership functions of the various losses caused by uneven foundation settlement (e_{26}) as {0, 0, 0, 0}, and the comparison results are shown in Figure 11. The loss evaluation indicator that has the greatest impact on the risk grade of DFP construction is the construction-period delay caused by the construction risk. One of the reasons is that the standard value of the loss membership function for the delay time is largest when normalized. Also, the results can be interpreted via the data in the expert scoring results. The opinions of the experts are

TABLE 22: The comparison of results obtained by using five methods respectively.

Adopted method	Ranking of risk level assessment results
AHP and fuzzy mathematics used in Meng et al. (2020)	H1 (0.6544) > H2 (0.3450) > H3 (0.0006) > H4 (0.0001) > H5 (0.0000)
FER used in Wei et al. (2020)	H2 (0.2438) > H3(0.2391) > H4(0.2118) > H1(0.1968) > H5(0.1084)
FER used in Mokhtari et al. (2012)	H2 (0.2395) > H3 (0.2191) > H1 (0.1918) > H4 (0.1898) > H5 (0.1594)
Fuzzy reasoning approach used in an et al. (2011)	H2 (1.000) > H1 (0.000) = H3 (0.000) = H4 (0.000) = H5 (0.000)
ANP used in Liu et al. (2014)	H2 (0.3297) > H1 (0.3042) > H3 (0.1708) > H4 (0.1103) > H5 (0.0850)
FER used in this paper	H2 (0.2479) > H3 (0.2180) > H4 (0.2166) > H1 (0.1957) > H5 (0.1214)

TABLE 23: Risk classification criteria.

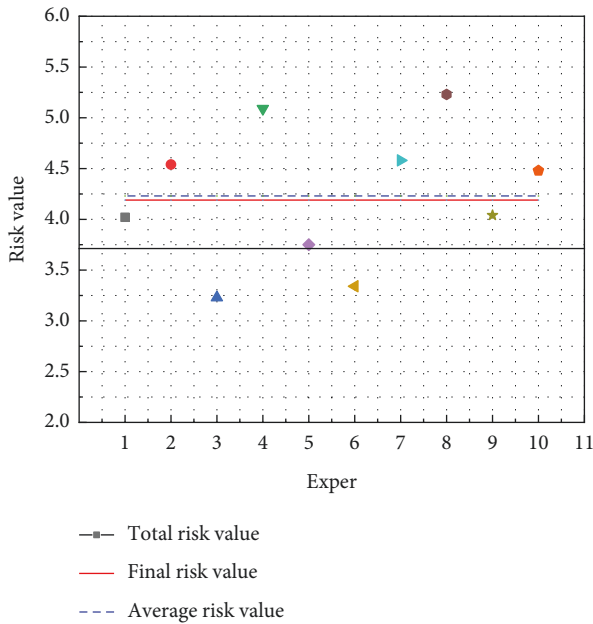| Grade	Risk value R	Acceptance	Disposal principle
Grade I	$1 < R$	Ignorable	Daily management and review
Grade II	$5 < R$	Permissible	Need to pay attention to strengthen the daily management review
Grade III	$10 < R$	Acceptable	Attention should be paid to preventive and monitoring measures
Grade IV	$15 < R$	Unacceptable	Decision-making is required to specify control and early warning measures
Grade V	$20 < R$	Refuse to accept	Immediately stop, rectify, avoid or activate the plan

FIGURE 14: Total risk value of each expert.

foundation pit instability due to an earthquake on H_1 and H_5 vary greatly. These are also the risk events with the largest weights. The changes in the basic belief grade before and after considering the weights of different risk events are compared in Figure 13, which shows that the changes in the basic belief of each risk event are basically the same, indicating that the impact on the distribution of basic belief is relatively small but cannot be ignored. Whether to consider risk loss indicator weights and risk event weights will impact the distribution of basic belief, especially risk loss indicator weights, and thus influence the determination of the key focus events. Therefore, introducing loss indicator weights and risk event weights can more accurately identify the key events to focus on and improve the accuracy of the assessment.

The above sensitivity analysis shows that we need to pay attention to the importance of risk event weights and risk loss indicator weights, focus on larger risk events and loss indicators, and exclude some extreme loss indicator evaluations.

7.2. Comparison with Previous Studies. The effectiveness of the method proposed herein is verified in comparison with five previously proposed risk-assessment methods, i.e., (i) the AHP and fuzzy mathematics due to Meng et al. [1], (ii) the FER method due to Wei et al. [10], (iii) the ANP method due to Liu et al. [29], (iv) the FER method due to Mokhtari et al. [30], and (v) the fuzzy reasoning approach due to An et al. [31].

The membership function for each risk level used in the fuzzy reasoning approach is not based on the likelihood of occurrence multiplied by the severity of the consequences, rather it depends on the domain knowledge of the risk expert involved. Although Mokhtari et al. [30] also used the FER method, their method for determining the belief structure differs from that used herein; they relied on the maximum ordinate value of the intersection point of the risk

widely divergent on the delay time loss index, and there are too-high or too-low extreme end evaluations. Therefore, if there are too-high or too-low evaluations in the scoring table, then consider removing these extreme evaluation data to make of the data as reasonable as possible.

Next, we analyze the basic belief distribution.

(5) The degree of change of the basic belief distribution function σ_n for each risk event before and after considering different loss indicator weights is compared. The results are presented in Figure 12, which shows that the basic belief σ_1^1 for hole collapse on H_1, the basic belief σ_5^6 for foundation treatment settlement on H_5, and the basic beliefs σ_1^{22} and σ_5^{22} for

membership function and the risk-identification framework, and the expert weights and risk factor weights are determined differently. The AHP and fuzzy mathematics method due to Meng et al. [1] uses membership functions to optimize the evaluation criteria of risk events, and it uses the AHP to calculate the risk. The FER method due to Wei et al. [10] uses the AHP to determine the weight of risk factors, but it does not fully consider a variety of loss indicators and their weights. The ANP method due to Liu et al. [29] conducts construction risk assessment by establishing a fuzzy network analysis method integrating the Delphi method, fuzzy comprehensive evaluation, and network analysis. The above five methods were applied to the present case for risk assessment, and the probability of rating each risk level was obtained, as given in Table 22.

The reasons for the different results obtained by the five methods and the proposed one are analyzed as follows. The method due to An et al. [31] drops the values between the minimum and maximum ones in the inference process, which makes the confidence level of the risk assessment result equal to one for a certain level, but it does not give the confidence level for each risk level. The FER method due to Mokhtari et al. [30] and Wei et al. [10] has the following discrepancies with the one proposed herein. (1) The difference between the proposed method and that due to Mokhtari et al. [30] comes from how the belief structure is determined. The probability gap between the top two risk levels with the highest probability of evaluation is $d_{23} = 0.2395 - 0.2191 = 0.0204$, $\overline{d_{23}} = 2479 - 0.218 = 0.0299$ (results of the proposed method in this study), $d_{23} < \overline{d_{23}}$. Therefore, it is better to use the area of intersection of the risk membership function and the risk-identification framework to determine the affiliation degree. (2) The difference between the proposed method and that due to Wei et al. [10] comes from how the expert weights are determined and the degree of perfection of the loss indicators. In this case, we have $d_{23} = 0.2438 - 0.2391 = 0.0047 < \overline{d_{23}}$, and so the proposed method can indicate the risk level more clearly. The reasonable determination of expert weights and perfect risk loss indicators are also important factors affecting the evaluation results. In the ANP method due to Liu et al. [29], the elements in the judgment matrix are expressed on a scale of 1–9. However, because of the inherent complexity and uncertainty of the DFP-construction risk problem, it is difficult for experts to express their preference with full confidence in the value. In this case, we have $d_{21} = 0.3297 - 0.3042 = 0.0255 < \overline{d_{23}}$, so the optimal evaluation result is not obtained.

It is noted that with the method due to Meng et al. [1], it is necessary to combine the risk levels in this study (Table 23) and establish the distribution curves of risk affiliation functions from level 1 to level 5 such as equations (26)–(30) , which is applied to the risk assessment of Jiangqiao station on Line 5 of the Nanning Metro. Using AHP, we obtain the risk evaluation value of each expert for the project (Figure 14). The overall risk value is 4.19, and the membership degree of each risk level is obtained by substituting into the membership function of each risk level equations (26)–(30), i.e., (0.55/4.19), (0.29/4.19), (4.7E − 04/4.19), (2.8E − 09/4.19), (6.6E − 10/4.19), and after normalization, we obtain the probability of the construction being rated as having a grade-I risk as being 65.44%. Compared with other methods, the results obtained are too risky, and there have been risk events in the actual construction process, such as water inflow from the catchment well and leakage of the enclosure structure; it is not enough to just carry out daily management and review. Also, as with ANP, AHP is not effective in avoiding information loss or distortion.

$$\mu_A(x_5) = \begin{cases} e^{-\left((x_5 - 22.5)/3\right)^2}, & 1 \le x_5 \le 22.5, \\ 1, & 22.5 \le x_1 \le 25, \end{cases} \tag{26}$$

$$\mu_A(x_4) = e^{-\left((x_4 - 17.5)/3\right)^2}, \; 1 \le x_4 \le 25, \tag{27}$$

$$\mu_A(x_3) = e^{-\left((x_3 - 12.5)/3\right)^2}, \; 1 \le x_3 \le 25, \tag{28}$$

$$\mu_A(x_2) = e^{-\left((x_2 - 7.5)/3\right)^2}, \; 1 \le x_2 \le 25, \tag{29}$$

$$\mu_A(x_1) = \begin{cases} 1, & 1 \le x_1 \le 3, \\ e^{-\left((x_1 - 3)/2.4\right)^2}, & 3 \le x_1 \le 25. \end{cases} \tag{30}$$

8. Conclusions

To overcome the limitation of single loss indicators in the existing risk-assessment methods of using FER to assess metro DFPs and the inherent defect of AHP to determine the risk weights, proposed herein was a risk-assessment evaluation model for metro DFP construction based on FER and TL-ANP. The validity of the model was verified by taking the construction risk evaluation of the descending Jiangqiao station on Line 5 of Nanning Metro as an example. We draw the following conclusions.

This study completed the risk loss evaluation indicators by normalizing the membership functions of different grades in the evaluation indicators, subdividing the risk loss into four indicators, and distributing weights to these indicators to avoid the influence of extreme evaluation on the final result, thereby making the assessment result of risk loss more objective.

For determining the weights, TL-ANP was applied to analyze the loss-indicator weights and risk-event weights in this study, which overcomes the problem of information loss in the continuous domain. GITrF-BWM was used to

reasonably determine the expert weights, which provides a quantitative basis for improving the reliability of the evaluation results.

Data Availability

The data used to support the findings of this study are currently under embargo while the research findings are commercialized. Requests for data, 12 months after publication of this article, will be considered by the corresponding author.

Conflicts of Interest

The authors declare that they have no conflicts of interest.

Acknowledgments

References

[1] G. Meng, J. Huang, B. Wu, Y. Zhu, S. Xu, and J. Hao, "Risk assessment of deep foundation pit construction based on analytic hierarchy process and fuzzy mathematics," *Advances in Civil Engineering*, vol. 2020, pp. 1–12, 2020.

[2] C. Zhou, T. Kong, S. Jiang, S. Chen, Y. Zhou, and L. Ding, "Quantifying the evolution of settlement risk for surrounding environments in underground construction via complex network analysis," *Tunnelling and Underground Space Technology*, vol. 103, Article ID 103490, 2020.

[3] H. Zhou, Y. Zhao, Q. Shen, L. Yang, and H. Cai, "Risk assessment and management via multi-source information fusion for undersea tunnel construction," *Automation in Construction*, vol. 111, Article ID 103050, 2020.

[4] M. An, Y. Chen, and C. J. Baker, "A fuzzy reasoning and fuzzy-analytical hierarchy process based approach to the process of railway risk information: a railway risk management system," *Information Sciences*, vol. 181, no. 18, pp. 3946–3966, 2011.

[5] S. Pender, "Managing incomplete knowledge: why risk management is not sufficient," *International Journal of Project Management*, vol. 19, no. 2, pp. 79–87, 2001.

[6] Z. Z. Wang and C. Chen, "Fuzzy comprehensive Bayesian network-based safety risk assessment for metro construction projects," *Tunnelling and Underground Space Technology*, vol. 70, pp. 330–342, 2017.

[7] S. Wan, J. Dong, and S.-M. Chen, "Fuzzy best-worst method based on generalized interval-valued trapezoidal fuzzy numbers for multi-criteria decision-making," *Information Sciences*, vol. 573, pp. 493–518, 2021.

[8] J. Jiang, X. Li, L. Xing, and YW Chen, "System risk analysis and evaluation approach based on fuzzy evidential reasoning," *Systems Engineering-Theory & Practice*, vol. 33, no. 2, pp. 529–537, 2013.

[9] X. Du, X. Zhang, M. Zhang, and B. Hou, "Risk synthetic assessment for deep pit construction based on evidence theory," *Chinese Journal of Geotechnical Engineering*, vol. 36, no. 1, pp. 155–161, 2014.

[10] D. Wei, D. Xu, and Y. Zhang, "A fuzzy evidential reasoning-based approach for risk assessment of deep foundation pit," *Tunnelling and Underground Space Technology*, vol. 97, Article ID 103232, 2020.

[11] F. W. Li, X. L. Du, M. J. Zhang, and Y.-H. Gao, "Application of improved AHP in risk identification during open-cut construction of a subway station," *Journal of Beijing University of Technology*, vol. 38, no. 2, pp. 167–172, 2012.

[12] X. Xin, P. Wan, and Y.-s. Shen, "Risk assessment of construction of excavations in areas of rock and soil," *Chinese Journal of Geotechnical Engineering*, vol. 34, pp. 343–346, 2012.

[13] H. Zhou and P. Cao, "A fuzzy AHP approach to select supporting schemes for city foundation pit in soft soil," *Journal of Central South University of Science and Technology*, vol. 43, no. 9, pp. 3582–3588, 2012.

[14] X. H. Bao, F. U. Yan-Bin, and H. W. Huang, "Case study of risk assessment for safe grade of deep excavations," *Chinese Journal of Geotechnical Engineering*, vol. 36, pp. 192–197, 2014.

[15] C. Xu and Q. Ren, "Fuzzy-synthetical evaluation on stability of surrounding rockmasses of underground engineering," *Chinese Journal of Rock Mechanics and Engineering*, vol. 23, no. 11, pp. 1852-1853, 2004.

[16] S. P. Wan, G. L. Xu, and J. Y. Dong, "Supplier selection using ANP and ELECTRE II in interval 2-tuple linguistic environment," *Information Sciences*, vol. 385, pp. 19–38, 2017.

[17] L. A. Zadeh, "Fuzzy sets," *Information and Control*, vol. 8, no. 3, pp. 338–353, 1965.

[18] J. Liu, J. B. Yang, J. Wang, and H. S. Sii, "Engineering system safety analysis and synthesis using the fuzzy rule-based evidential reasoning approach," *Quality and Reliability Engineering International*, vol. 21, no. 4, pp. 387–411, 2005.

[19] J. B. Yang, Y. M. Wang, D. L. Xu, and K. Chin, "The evidential reasoning approach for MADA under both probabilistic and fuzzy uncertainties," *European Journal of Operational Research*, vol. 171, no. 1, pp. 309–343, 2006.

[20] L. Martinez and F. Herrera, "A 2-tuple fuzzy linguistic representation model for computing with words," *IEEE Transactions on Fuzzy Systems*, vol. 8, no. 6, pp. 746–752, 2000.

[21] C. T. Chen and W. S. Tai, "Measuring the intellectual capital performance based on 2-tuple fuzzy linguistic information," *Proceedings of the 10th Annual Meeting of Asia Pacific Region of Decision Sciences Iinstitute*, Taiwan, 2005.

[22] G. Büyüközkan and G. Çifçi, "A novel hybrid MCDM approach based on fuzzy DEMATEL, fuzzy ANP and fuzzy TOPSIS to evaluate green suppliers," *Expert Systems with Applications*, vol. 39, no. 3, pp. 3000–3011, 2012.

[23] J. Rezaei, "Best-worst multi-criteria decision-making method: some properties and a linear model," *Omega*, vol. 64, pp. 126–130, 2016.

[24] J. Rezaei, "Best-worst multi-criteria decision-making method," *Omega*, vol. 53, pp. 49–57, 2015.

[25] H. H. Choi, H. N. Cho, and J. W. Seo, "Risk assessment methodology for underground construction projects," *Journal of Construction Engineering and Management*, vol. 130, no. 2, pp. 258–272, 2004.

[26] A. Valipour, N. Yahaya, N. Md Noor, J. Antuchevičienė, and J. Tamošaitienė, "Hybrid SWARA-COPRAS method for risk assessment in deep foundation excavation project: an Iranian case study," *Journal of Civil Engineering and Management*, vol. 23, no. 4, pp. 524–532, 2017.

[27] H.-b. Zhou and H. Zhang, "Risk assessment methodology for a deep foundation pit construction project in shanghai,

China," *Journal of Construction Engineering and Management*, vol. 137, no. 12, pp. 1185–1194, 2011.

[28] J. B. Jian-Bo Yang and D. L. Dong-Ling Xu, "On the evidential reasoning algorithm for multiple attribute decision analysis under uncertainty," *IEEE Transactions on Systems, Man, and Cybernetics - Part A: Systems and Humans*, vol. 32, no. 3, pp. 289–304, 2002.

[29] B. Liu, M. Shen, and Q. Ma, "Application of fuzzy analytic network process in risk analysis for construction of highway mountain tunnel," *Chinese Journal of Rock Mechanics and Engineering*, vol. 33, pp. 2861–2869, 2014.

[30] K. Mokhtari, J. Ren, C. Roberts, and J. Wang, "Decision support framework for risk management on sea ports and terminals using fuzzy set theory and evidential reasoning approach," *Expert Systems with Applications*, vol. 39, no. 5, pp. 5087–5103, 2012.

[31] M. An, Y. Chen, and C. J. Baker, "A fuzzy reasoning and fuzzy-analytical hierarchy process based approach to the process of railway risk information: a railway risk management system," *Information Sciences*, vol. 181, no. 18, pp. 3946–3966, 2011.